

# Fast Randomized Singular Value Thresholding for Nuclear Norm Minimization

Tae-Hyun Oh *Student Member, IEEE*, Yasuyuki Matsushita, Yu-Wing Tai *Senior Members, IEEE*,  
and In So Kweon *Member, IEEE*

**Abstract**—Rank minimization can be boiled down to tractable surrogate problems, such as Nuclear Norm Minimization (NNM) and Weighted NNM (WNNM). The problems related to NNM (or WNNM) can be solved iteratively by applying a closed-form proximal operator, called Singular Value Thresholding (SVT) (or Weighted SVT), but they suffer from high computational cost of computing Singular Value Decomposition (SVD) at each iteration. We propose a fast and accurate approximation method for SVT, that we call fast randomized SVT (FRSVT), where we avoid direct computation of SVD. The key idea is to extract an approximate basis for the range of a matrix from its compressed matrix. Given the basis, we compute the partial singular values of the original matrix from a small factored matrix. In addition, by adopting a range propagation technique, our method further speeds up the extraction of approximate basis at each iteration. Our theoretical analysis shows the relationship between the approximation bound of SVD and its effect to NNM via SVT. Along with the analysis, our empirical results quantitatively and qualitatively show that our approximation rarely harms the convergence of the host algorithms. We assess the efficiency and accuracy of our method on various vision problems, *e.g.*, subspace clustering, weather artifact removal, and simultaneous multi-image alignment and rectification.

**Index Terms**—Singular value thresholding, rank minimization, nuclear norm minimization, robust principal component analysis, low-rank approximation



## 1 INTRODUCTION

Low-rank matrix recovery arises in many engineering and applied science problems, and rank minimization techniques have attracted tremendous interests. Rank minimization is a crucial regularizer to derive a low-rank solution and is needed in many mathematical models in computer vision and machine learning [4], [9], [13], [20], [22], [27], [29], [30], [32], [37], [39]. As rank minimization,  $\min \text{rank}(\mathbf{X})$  s.t.  $\mathbf{X} \in \mathcal{C}$ , is generally an NP-hard problem, it is typically relaxed using the nuclear norm (*i.e.*,  $\|\cdot\|_*$ , the sum of the singular values), which is the convex surrogate for the rank function  $\text{rank}(\cdot)$ .

A nuclear norm minimization (NNM) problem is expressed as

$$\mathbf{X}^* = \underset{\mathbf{X}}{\text{argmin}} f(\mathbf{X}) + \tau \|\mathbf{X}\|_*, \quad (1)$$

where  $\mathbf{X} \in \mathbb{R}^{m \times n}$ , and  $\tau > 0$  is a regularization parameter. The function  $f(\mathbf{X})$  can be arbitrarily defined depending on the objectives, *e.g.*,  $f(\mathbf{X}) = \|\mathbf{O} - \mathbf{X}\|_1$  in robust principal component analysis (RPCA) [3],  $f(\mathbf{X}) = \frac{1}{2} \|\mathbf{A}\mathbf{X} - \mathbf{B}\|_F^2$  in multivariate regression and multi-class learning [25], and  $f(\mathbf{X}) = \frac{1}{2} \|\pi_\Psi(\mathbf{O}) - \pi_\Psi(\mathbf{X})\|_F^2$  in matrix completion [3]. Here,  $\mathbf{O}$  is measured data,  $\|\cdot\|_1$  and  $\|\cdot\|_F$  denote  $l_1$  and Frobenius norms, and  $\pi_\Psi(\cdot)$  is an orthogonal projection operator setting  $[\pi_\Psi(\mathbf{X})]_{i,j} = [\mathbf{X}]_{i,j}$  for  $(i,j) \in \Psi$  and 0 otherwise. Weighted nuclear norm minimization (WNNM), which could be non-convex depending on the weights [9], [13], [28], can alternatively be used to better approximate the original rank function  $\text{rank}(\cdot)$ .

Unless the loss function  $f(\mathbf{X})$  is a proximity term, most previous works use first-order optimization approaches, *e.g.*, dual method [7], accelerated proximal gradient [14], augmented Lagrange multiplier (ALM) [17], alternating direction method (ADM) [17], [18], and iteratively reweighted least-squares [23]. All these approaches, *i.e.*, NNM, WNNM, and their regularized versions, iteratively solve a simple NNM sub-problem defined as the following nuclear norm and proximity terms:

**Problem (Nuclear norm minimization).** For  $\tau \geq 0$  and  $\mathbf{A} \in \mathbb{R}^{m \times n}$ ,

$$\mathbf{X}^* = \underset{\mathbf{X}}{\text{argmin}} \tau \|\mathbf{X}\|_* + \frac{1}{2} \|\mathbf{X} - \mathbf{A}\|_F^2, \quad (2)$$

where optimal  $\mathbf{X}^*$  can be obtained by the singular value thresholding operator defined as following.

**Definition 1 (Singular value thresholding<sup>1</sup> [1]).** The problem (2) has a closed-form solution given by the singular value thresholding (SVT) operator  $\mathbb{S}_\tau(\cdot)$  as

$$\mathbf{X}^* = \mathbb{S}_\tau(\mathbf{A}) = \mathbf{U}_\mathbf{A} \mathcal{S}_\tau(\Sigma_\mathbf{A}) \mathbf{V}_\mathbf{A}^\top, \quad (3)$$

where  $\mathcal{S}_\tau(x) = \text{sgn}(x) \cdot \max(|x| - \tau, 0)$  is the soft shrinkage operator [10], and  $\mathbf{U}_\mathbf{A} \Sigma_\mathbf{A} \mathbf{V}_\mathbf{A}^\top$  is the SVD of  $\mathbf{A}$ .

The major computational bottleneck of NNM and WNNM problems is the necessity of solving Eq. (2) multiple times, where SVD computation occupies the largest computation cost (*e.g.*,  $O(mn \min(m, n))$  for each SVD [8]).

This paper proposes a fast SVT technique to accelerate general NNM and WNNM methods. Our method is motivated by the previous study of a randomized SVD proposed by Halko *et al.* [11], and we extend the original general method in several respects for better solving the NNM and WNNM problems

1. A similar result for WNNM can be found in [9], called WSVT.

- T.-H. Oh, Y.-W. Tai, and I.S. Kweon (corresponding author) are with the Department of Electrical Engineering, KAIST, Daejeon, Republic of Korea. E-mail: thoh.kaist.ac.kr@gmail.com, yuwing@gmail.com and iskweon77@kaist.ac.kr
- Y. Matsushita is with Osaka University, Osaka, Japan. E-mail: yasumat@ist.osaka-u.ac.jp

Manuscript received April 19, 2005; revised September 17, 2014.

$\pi_{\Psi}(\cdot)$	Orthogonal projection operator with a map (index set) $\Psi$
$\mathbb{S}_{\tau}(\cdot)$	SVT operator [1] with the parameter $\tau$
$\mathcal{S}_{\tau}(\cdot)$	Soft shrinkage operator [10] with the parameter $\tau$
$\sigma_i(\cdot)$	$i$ -th singular value of a matrix
$\Omega$	A standard Gaussian random matrix
$\mathbf{Q}$	Orthonormal column matrix
$\mathbf{O}$	Observation matrix (Input)
$\mathbf{L}, \mathcal{L}$	Low-rank optimization related matrix or tensor
$\mathbf{S}, \mathcal{E}$	Sparse optimization related matrix or tensor
$k$	Parameter for the target rank
$p$	Parameter for over-sampling rate
$l$	Sampling (predicted) rate ( $l = k + p$ )
$r$	True rank of the target matrix $\mathbf{A}$
$s$	Real sampling rate ( $s = \min(l, r)$ )
$\eta$	Number of the power iteration
$b$	Parameter for the maximum rank bound
$\mathbf{v}$	Parameter vector for the polynomial error bound ( $\mathbf{v} = \{k, p\}$ without the power iteration, or $\mathbf{v} = \{k, p, \eta\}$ with it)

TABLE 1: Summary of notations

that we focus on in this paper. As a result, we propose an algorithm that we call *fast randomized SVT* (FRSVT). We present the connection between FRSVT and low-rank approximation with both theoretical and empirical analyses, and show the effectiveness of the proposed method via simulations and a few applications. Specifically, this paper makes the following contributions:

- We develop a successive truncated low-rank decomposition that can be generally applied to NNM and WNNM problems. Our method achieves high efficiency without degrading the accuracy of the host algorithms.
- By exploiting the proximity of the range space over iterations, our method propagates the estimated basis at the previous iteration to the next one for acceleration. We call this technique *range propagation* (RP).
- We provide a theoretical analysis between the low-rank approximation and our FRSVT method. In addition, we show the empirical stability and behavior of our method with respect to varying parameters.
- We apply FRSVT to various computer vision applications and show the performance gain in comparison with previous methods.

A preliminary version of this paper has appeared in [31]. We extend [31] by analyzing the behaviors of our algorithm in both theoretical and empirical aspects as follows. The detail approximation bound derivation, exactness condition and comparison with LTSVD and our baseline are newly supplemented in Sec. 3. Based on the analyses, we provide implementation tips and other options that can potentially improve the performance of the proposed algorithm. Additional simulation and experimental results are supplemented in Sec. 4. Table 1 summarizes the notation used in the rest of the paper.

## 1.1 Related Works

Candès *et al.* [3] showed that, under some mild condition, the solution of NNM is equivalent to the solution of rank minimization in conjunction with a sparse outlier model [3]. Inspired by the success of this convex surrogate for rank minimization, low-rank structures have been exploited in various computer vision applications, such as rain removal [4], denoising [9], inpainting [13], motion segmentation by subspace clustering [20], structure from motion [22], background sub-

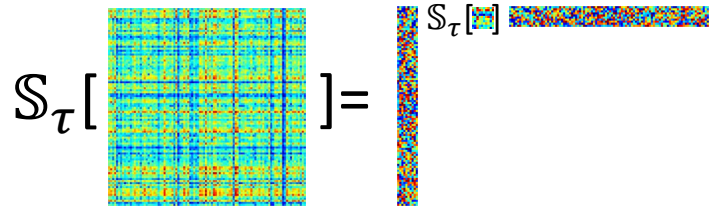


Fig. 1: Basic idea of our method. Instead of applying SVT to the large original matrix, if we can obtain the same result by applying SVT to small matrix with few additional efforts, the complexity could be significantly drop. As shown in Proposition 1, once a large matrix is decomposed into a core matrix and orthonormal matrices (the left and right thin matrices in the illustration), by applying SVT to the small core matrix we can obtain the same result with the one obtained from direct SVT computation on the large matrix.

traction [27], tag transduction [27], high dynamic range imaging [30], batch image alignment [32], photometric stereo [37], image rectification [39], and nuclear norm regularized learning [25].

While useful, due to the high computational complexity of NNM, namely, SVD used in the SVT operator, a fast SVT method has always been wanted in both small- and large-scale problems. Liu *et al.* [21] efficiently solve NNM by factorizing the original matrix into two small matrices. Although the work achieved significant speed-up, global optimum cannot be guaranteed due to that the factorization introduces non-convexity like other factorization methods [6], [40].

With retaining the advantage of convexity, Liu *et al.* [22] exactly solve RPCA on a small sub-sampled matrix and propagate the seed solution to other parts via  $\ell_1$  filtering. Since the work focuses only on RPCA problem but not general NNM problems, a fast and general SVT method is still needed as a tool for NNM to be applied to large-scale problems. Cai *et al.* [2] avoid explicit SVD computation using the dual of SVT. Since their method uses Newton iterations with an inverse matrix, the input matrix needs to be preprocessed by the complete orthogonal decomposition [8] (COD) to ensure a non-singular square matrix. The standard COD consists of twice of QR decompositions with column/row pivoting, which requires  $O(mn \min(m, n))$ ; therefore, the reduction of computation complexity is still limited.

In other thread of works, it has been shown that the exact SVD computation is unnecessary in the inner loop of NNM. Mu *et al.* [27] propose a compressed optimization by random projection. Ma *et al.* [25] solve NNM related problems with a linear-time approximate SVD [5]. However, these methods become occasionally unstable, because the input matrix is directly approximated by sampling or projection in the methods, where the original information is impaired, and the randomness leads to unstable and incorrect results. Unlike these methods, our method only approximates the subspace bases to guarantee that most spectrum information is retained.

## 2 FAST RANDOMIZED SINGULAR VALUE THRESHOLDING (FRSVT)

The basic idea of our method shares the idea of Liu *et al.* [22] and Ma *et al.* [25], in that the solution of Eq. (2) can be found by applying SVT to a small matrix instead of the original large matrix as illustrated in Fig. 1. Instead of sampling columns or rows of a matrix as in [22], [25], our method extracts a small core matrix by finding orthonormal bases with the

unitary invariant property. Specifically, since the NNM defined in Eq. (2) consists of unitary invariant norms, the following equality holds:

**Proposition 1.** Let  $\mathbf{A} = \mathbf{Q}\mathbf{B} \in \mathbb{R}^{m \times n}$ , where  $\mathbf{Q} \in \mathbb{R}^{m \times n}$  has orthonormal columns. Then,

$$\mathbb{S}_\tau(\mathbf{A}) = \mathbf{Q} \mathbb{S}_\tau(\mathbf{B}), \quad (4)$$

where  $\mathbb{S}_\tau(\cdot)$  is the SVT operator.

*Proof.* When  $m = n$  and  $\mathbf{Q}$  is an orthonormal matrix, the equality obviously holds by the unitary invariant property of norms. For  $m > n$ , we prove the equality for the orthonormal column matrix. Consider an arbitrary matrix  $\mathbf{Z} = \mathbf{U}_Z \Sigma_Z \mathbf{V}_Z^\top \in \mathbb{R}^{n \times n}$ , where  $\mathbf{U}_Z \Sigma_Z \mathbf{V}_Z^\top$  is  $\mathbf{Z}$ 's SVD, then

$$\begin{aligned} \mathbf{Q} \cdot \mathbb{S}_\tau(\mathbf{B}) &= \mathbf{Q} \cdot \operatorname{argmin}_{\mathbf{Z}} \left( \tau \|\mathbf{Z}\|_* + \frac{1}{2} \|\mathbf{Z} - \mathbf{B}\|_F^2 \right) \\ &= \operatorname{argmin}_{\mathbf{X}} \left( \tau \|\mathbf{Q}^\top \mathbf{X}\|_* + \frac{1}{2} \|\mathbf{Q}(\mathbf{X} - \mathbf{B})\|_F^2 \right) \\ &\text{(by letting } \mathbf{Q}\mathbf{Z} = \mathbf{X}, \text{ and as } \mathbf{Q}^\top \mathbf{Q} = \mathbf{I}, \\ &\text{and the unitary invariant norm property)} \\ &= \operatorname{argmin}_{\mathbf{X}} \left( \tau \|\mathbf{X}\|_* + \frac{1}{2} \|\mathbf{X} - \mathbf{Q}\mathbf{B}\|_F^2 \right) \\ &\text{(since } \|\mathbf{Q}^\top \mathbf{X}\|_* = \|\mathbf{Z}\|_* = \|\mathbf{Q}\mathbf{Z}\|_* = \|\mathbf{X}\|_*) \\ &= \mathbb{S}_\tau(\mathbf{Q}\mathbf{B}) = \mathbb{S}_\tau(\mathbf{A}). \end{aligned}$$

□

In general, SVT requires SVD computation, and its complexity<sup>2</sup> is  $O(mn^2)$ . Based on Proposition 1, we can avoid expensive computation by instead computing SVT on a smaller matrix  $\mathbf{B} \in \mathbb{R}^{n \times n}$  when  $\mathbf{Q} \in \mathbb{R}^{m \times n}$  is available. Given  $\mathbf{Q} \in \mathbb{R}^{m \times k}$  that best approximates  $\mathbf{A}$  by a rank- $k$  matrix, the complexity of SVD of  $\mathbf{B} \in \mathbb{R}^{k \times n}$  becomes  $O(nk^2)$ . Therefore, when  $k \ll n$ , the computation speed can be significantly improved.

Our SVT computation iterates the following two steps: 1) Estimating an orthonormal column matrix  $\mathbf{Q}$ , and 2) Computing SVD of  $\mathbf{B}$  for SVT. For SVT computation, a partial (or truncated) SVD is frequently used to reduce the complexity in many prior arts. Our method similarly finds a rank- $k$  approximation ( $k < n$ ) of the original matrix  $\mathbf{A}$  as  $\mathbf{A} \approx \hat{\mathbf{A}}_k = \mathbf{Q}\mathbf{B}$ . It saves the computation of the first step as well as the second step, because the size of matrices  $\mathbf{Q}$  and  $\mathbf{B}$  are reduced to  $m \times k$  and  $k \times n$ , respectively. By exploiting the observation that the major orthonormal  $k$  bases evolve slowly over iterations, our method efficiently initializes matrix  $\mathbf{Q}$  at each iteration by bypassing expensive random range estimation (Range propagation in Sec. 2.1). In addition, by avoiding direct SVD computation, we can further reduce the computation as described in Sec. 2.2. Also, we describe a target rank prediction technique for further improving speed in Sec. 2.3.

## 2.1 Finding Approximate Range

Inspired by Halko *et al.* [11], we first estimate the orthonormal bases  $\mathbf{Q} = [\mathbf{q}_1, \dots, \mathbf{q}_l]$  (where  $l \geq k$ ) such that  $\operatorname{span}(\mathbf{Q}) \subseteq \operatorname{Range}(\mathbf{A})$  from a matrix compressed by random projection. Intuition of their randomized range finding algorithm is as follows. By multiplying a random vector  $\omega_j$ , a

2. Without loss of generality, we assume  $m \geq n$  in this paper. In the case  $m < n$ , the proposed method is analogous.

## Algorithm 1 Fast Randomized Singular Value Thresholding (FRSVT) algorithm

**Input :**  $\mathbf{A} \in \mathbb{R}^{m \times n}, \tau > 0, l = k + p > 0$  and  $q \geq 0$ . For range propagation, the orthonormal column matrix  $\tilde{\mathbf{Q}}$  of the previous iteration.

**if not** Range propagation **then**

Sample Gaussian random matrix  $\Omega \in \mathbb{R}^{n \times l}$

$\mathbf{Y} = \mathbf{A}\Omega$

$\mathbf{Q} = \text{QR\_CP}(\mathbf{Y})$

**else**

Sample Gaussian random matrix  $\Omega \in \mathbb{R}^{n \times p}$

$\mathbf{Y} = \mathbf{A}\Omega$

$\mathbf{Q}_Y = \text{PartialOrthogonalization}(\tilde{\mathbf{Q}}, \mathbf{Y})$

$\mathbf{Q} = [\tilde{\mathbf{Q}}, \mathbf{Q}_Y]$

**end if**

**repeat**

$\mathbf{Q} = \text{QR}(\mathbf{A}\mathbf{A}^\top \mathbf{Q})$

**until**  $\eta$  times

$[\mathbf{H}, \mathbf{C}] = \text{QR}(\mathbf{A}^\top \mathbf{Q})$

$[\mathbf{W}, \mathbf{P}] = \text{PolarDecomposition}(\mathbf{C})$

$[\mathbf{V}, \mathbf{D}] = \text{EigenDecomposition}(\mathbf{P})$

$\mathbb{S}_\tau(\mathbf{A}) = (\mathbf{Q}\mathbf{V}) \mathbb{S}_\tau(\mathbf{D}) (\mathbf{H}\mathbf{W}\mathbf{V})^\top$

**Output :**  $\mathbb{S}_\tau(\mathbf{A}), \tilde{\mathbf{Q}} = \mathbf{Q}\mathbf{V}$

random linear combination  $\mathbf{y}_j$  of the column vectors of  $\mathbf{A}$  is generated, which encodes the partial range of  $\mathbf{A}$ . Suppose  $\mathbf{A} = \mathbf{A}_k + \mathbf{E}$ , where  $\mathbf{A}_k$  is the rank- $k$  projection of  $\mathbf{A}$ , whose range is the target to be captured, and  $\mathbf{E}$  represents small perturbation, then sample vector  $\mathbf{y}_j$  can be obtained by

$$\mathbf{y}_j = \mathbf{A}_k \omega_j + \mathbf{E} \omega_j. \quad (5)$$

Even though unwanted  $\mathbf{E}$  may be included in  $\{\mathbf{y}_j\}$  because the action of  $\mathbf{A}_k$  (*i.e.*, magnitudes of spectrum) is larger than  $\mathbf{E}$ , the range of  $\mathbf{A}_k$  is dominant to be captured in  $\{\mathbf{y}_j\}$ . However, if only  $k$  vectors  $\{\mathbf{y}_j\}$  are sampled,  $\{\mathbf{y}_j\}$  could not span the entire  $\operatorname{Range}(\mathbf{A}_k)$ . By increasing the sampling rate, most of  $\operatorname{Range}(\mathbf{A}_k)$  can be captured; therefore, we oversample  $l$  sample vectors, so that  $\operatorname{Range}(\mathbf{A}_k)$  can be captured as much as possible.

Given the sample matrix  $\mathbf{Y} = [\mathbf{y}_1, \dots, \mathbf{y}_l]$ , where  $l = k + p$ ,  $\mathbf{Q}$  can be obtained by orthonormalizing  $\mathbf{Y}$ . When  $r = \operatorname{rank}(\mathbf{A}) < l$ ,  $r$  bases are enough to span the entire  $\operatorname{Range}(\mathbf{A})$ . Indeed, when  $\operatorname{rank}(\mathbf{A}) < l$ , the range finding algorithm is fairly accurate and close to the exact method as we will see the theoretical analysis in Sec. 3. Thus, we can reduce the dimension of  $\mathbf{Q}$  for almost free by estimating the rank and dominant bases by QR decomposition with Column Pivoting (QR-CP) to  $\mathbf{Y}$ . While Halko *et al.* also proposed an algorithm to adaptively and approximately determine the number of bases by different randomization for sampling, orthogonalization, and re-orthogonalization, our method is based on an exact method with the same complexity using QR-CP, and we adaptively predict the sampling rate in a simpler manner (we will see in Sec. 2.3). Fortunately, in LAPACK, an efficient QR-CP routine using level-3 BLAS (`dgeqp3`) is available. Moreover, our method does not require the upper triangle matrix from QR, but only the orthonormal basis  $\mathbf{Q}$ ; therefore, we can avoid extracting the whole triangular matrix but only compute rank and  $\mathbf{Q}$  with `dgeqp3` and `orgqr` routines, respectively. After obtaining  $\mathbf{Q} \in \mathbb{R}^{m \times s}$ , where  $s = \min(l, r)$ , we can compute a small matrix  $\mathbf{B}$  by  $\mathbf{B} = \mathbf{Q}^\top \mathbf{A} \in \mathbb{R}^{s \times n}$ .

**Range Propagation (RP) for Fast Range Finding** Based on the observation that  $\operatorname{Range}(\mathbf{A}_{(i)})$  at the  $i$ -th iteration is similar to the one at the  $(i - 1)$ -th iteration in NNM related

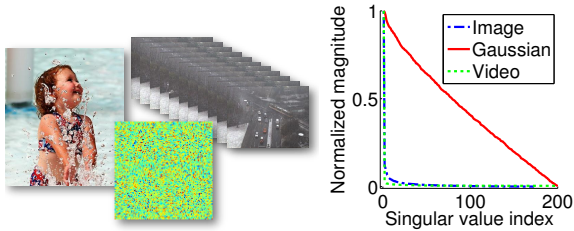


Fig. 2: Illustration of singular value decaying. [Left] Gaussian random, video and image samples. [Right] Decaying graphs of singular values. The Red, Green, Blue lines represent the graphs of a Gaussian random matrix, video, and image, respectively. The spectrum of visual data decays significantly fast.

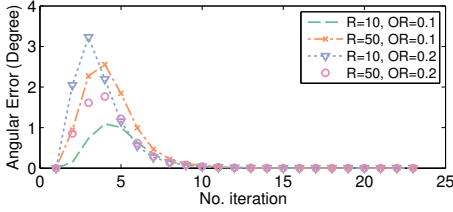


Fig. 3: Angular difference of subspaces between subsequent iterations.

problems, our method uses the singular vectors at the  $(i-1)$ -th step as an initial approximation of range bases  $\mathbf{Q}_{(i)}$  at the  $i$ -th step. To capture the change of the range space, we additionally sample  $p$  sample vectors  $\{\mathbf{y}\}$ . We append the sampled  $\{\mathbf{y}\}$  to the previous singular vector matrix  $\mathbf{Q}_{(i-1)}$  as  $\mathbf{Q}_{(i)} = [\hat{\mathbf{Q}}_{(i-1)}, \mathbf{y}_1, \dots, \mathbf{y}_p]$ , and apply partial orthogonalization only for newly added  $\{\mathbf{y}\}$  by a modified Gram-Schmidt procedure [8]. The number of bases can subsequently be reduced by checking the rank with QR-CP in the first step of the power iteration.

**Power Iteration** Among the overall process in our algorithm, since the only approximation step is estimation of the orthonormal column matrix  $\mathbf{Q}$ , the accuracy of our algorithm depends only on this step. In Eq. (5), if the magnitude of the action of  $\mathbf{A}_k$  is not dominant against  $\mathbf{E}$ , the directions of sample vectors are biased and may be included in  $\text{Range}(\mathbf{A}_k)^\perp$ . This introduces accuracy degradation to the rest of the process. To resolve this issue, Halko *et al.* [11] proposed a power iteration scheme, which makes the spectrum difference between  $\mathbf{A}_k$  and  $\mathbf{E}$  larger by estimating  $\mathbf{Q}$  on  $(\mathbf{A}\mathbf{A}^\top)^\eta \mathbf{A}$ . It improves the chance of better capturing the range of  $\mathbf{A}_k$  from  $\mathbf{Y} = (\mathbf{A}\mathbf{A}^\top)^\eta \mathbf{A}\Omega$ , while the singular vectors remain unchanged. Halko *et al.* also showed that  $\eta = 2$  or 4 power iterations are sufficient for usual data of interest, and highly accurate range finding can be achieved. As shown in Fig. 2, decay of singular values of visual data is much faster than a Gaussian random matrix. Our empirical tests also show that  $\eta = 2$  is sufficient, and it is used in all our experiments.

## 2.2 Computing the Singular Values (Vectors)

The NNM problem is now reduced to SVT on a smaller matrix  $\mathbf{B}$ . In this section, we further reduce the computation time of SVT on  $\mathbf{B}$ . The SVT operator can be computed by SVD and shrinkage on its singular values. For positive semi-definite matrices, SVD can be more efficiently computed by Eigen decomposition (ED), which is typically faster than SVD in our empirical tests with small matrices. To apply ED to a general matrix, we form a positive semi-definite matrix by the following decomposition:

**Definition 2 (Polar decomposition [12]).** Let  $\mathbf{X} \in \mathbb{C}^{m \times n}$ ,  $m \geq n$ . There exists a matrix  $\mathbf{W} \in \mathbb{C}^{m \times n}$  and a unique Hermitian positive semi-definite matrix  $\mathbf{P} \in \mathbb{C}^{n \times n}$  such that

$$\mathbf{X} = \mathbf{W}\mathbf{P}, \quad \mathbf{W}^* \mathbf{W} = \mathbf{I},$$

where  $\mathbf{I}$  is the identity matrix. If  $\text{rank}(\mathbf{X}) = n$ , then  $\mathbf{P}$  is positive definite and  $\mathbf{W}$  is uniquely determined.

Note that the existence of polar decomposition is equivalent to the existence of SVD.

We use a Newton based polar decomposition suggested by Higham *et al.* [12], which has a quadratic convergence behavior. In our experiment, it converges at a small number of iterations (typically, seven) with various different data, which is consistent with the result of [2], [12]. Due to the requirement of the inverse operator in Newton iterations, it is only applicable to non-singular square matrices. Since  $\mathbf{B}^\top \in \mathbb{R}^{n \times s}$  is a full column rank matrix, the non-singular square matrix can be simply obtained from  $\mathbf{B}^\top = \mathbf{H}\mathbf{C}$  by QR decomposition, where we call  $\mathbf{C} \in \mathbb{R}^{s \times s}$  a *core matrix* that is always non-singular and square. For this step, unlike the procedure in Sec. 2.1, no column pivoting is required.

We sequentially apply the polar decomposition and ED on the core matrix;  $\mathbf{C} = \mathbf{W}\mathbf{P} = \mathbf{W}\mathbf{V}\mathbf{D}\mathbf{V}^\top$ , where  $\mathbf{D}$  and  $\mathbf{V}$  are the eigenvalue and eigenvector matrices of  $\mathbf{P}$ , respectively. Since the matrices  $\mathbf{H}$ ,  $\mathbf{W}$ , and  $\mathbf{V}$  are orthonormal column matrices, the diagonal matrix  $\mathbf{D}$  is equivalent to the singular value matrix of  $\mathbf{B}$ . Finally,  $\mathcal{S}_\tau(\mathbf{A})$  can be approximated by

$$\mathcal{S}_\tau(\mathbf{A}) \approx \mathcal{S}_\tau(\hat{\mathbf{A}}_s) = (\mathbf{Q}\mathbf{V}) \mathcal{S}_\tau(\mathbf{D}) (\mathbf{H}\mathbf{W}\mathbf{V})^\top. \quad (6)$$

For the range propagation, the singular vector matrix  $\tilde{\mathbf{Q}}$  is stored as  $\tilde{\mathbf{Q}} = \mathbf{Q}\mathbf{V}$  or  $\mathbf{H}\mathbf{W}\mathbf{V}$  (according to the side of random matrix multiplication). Overall algorithm is summarized in Algorithm 1.

## 2.3 Adaptive Rank Prediction (AP) Heuristic

For SVT, only singular vectors corresponding to the singular values that are greater than a certain threshold are needed, and full SVD is unnecessary. Since the rank of  $\mathbf{A}_{(i)}$  is unknown before SVD, predicting its rank can avoid unnecessary computation. We observe that, in many NNM related problems, the rank of  $\mathbf{A}_{(i)}$  is monotonically increasing or decreasing over iterations, and the rank is stabilized as the number of iteration increases. As we shall see in the theorem of error bound in Sec. 3, over-sampling is always useful to reduce the expected error bound of FRSVT. Thus, optimistically predicting rank allows to achieve both computational efficiency and stability.

The efficiency of our method may be degraded by an excessively high sampling rate. In such a case, we resort to the truncated SVT by upper bounding the target rank. As shown in natural image statistics of Fig. 2, the rank of  $\mathbf{A}_{(i)}$  is generally stabilized at low-rank in many computer vision application. Usually, the final accuracy is not harmed, as seen in the successes of the truncated SVD in the NNM related problems [17], [18], [19], [21].

Based on these observations, we define over-sampling rate  $p$  as:

$$p_{i+1} = \begin{cases} a, & \text{if } r_i < l_i, \\ \lceil \rho n \rceil, & \text{otherwise,} \end{cases} \quad (7)$$

where  $m \geq n$  is assumed,  $a$  is a constant (set to  $a = 2$ ),  $\rho \in (0, 1]$  is a constant parameter to rapidly follow the real

rank  $r_i$  (set to  $\rho = 0.05$ ), and  $\lceil \cdot \rceil$  denotes the `ceil` operation. The prediction rule for sampling rate is defined as  $l_{i+1} = \min(r_i + p_{i+1}, b)$ , where  $b = \lceil \gamma n \rceil$  is the maximum bound of sampling rate,  $\gamma \in (0, 1]$  is the proportion parameter. The sampling rate  $l_i$  can be regarded as the predicted rank at the  $i$ -th iteration, and  $r_i$  is the number of singular values of  $\mathbf{A}_{(i)}$  that are larger than the threshold, *i.e.*, the estimated rank of  $\mathbb{S}_\tau(\mathbf{A}_{(i)})$ . Initially, we set  $l_0 = 0.1b$ . In the case of the range propagation, the number of columns in  $\hat{\mathbf{Q}}_{(i-1)}$  becomes  $r_i$ , and  $p_i = l_i - r_i$ .

When  $r_i < l_i$ , Eq. (7) slightly over-samples, otherwise it optimistically predicts the rank of the next iteration by the a larger over-sampling rate. By virtue of low-rankness of visual data shown in Fig. 2, the optimistic rule leads to an accurate estimate.

## 2.4 Fast Random Projection

We can replace the Gaussian random matrix with other less expensive and fast transforms according to the Johnson-Lindenstrauss lemma [26], such as a subsampled random Fourier transform, subsampled random Hadamard transform, or sparse random Gaussian matrix (in Matlab, `sprandn()` function). The cost of the sparse random Gaussian matrix transform depends on the sparsity of the matrix, but it may become less accurate if the matrix is too sparse. The two structured subsampled random matrices can be multiplied with the cost  $O(mn \log l)$  by efficient computation methodology (*e.g.*, FFT), while the cost of dense Gaussian matrix multiplication is  $O(mnl)$ . In our implementation, we simply use dense Gaussian random matrix drawn from standard normal distribution in entry-wise.

## 2.5 Computational Complexity

Although the computation of the sample matrix  $\mathbf{Y}$  by random projection requires  $O(mnl)$ , we can reduce it to  $O(mn)$  by the range propagation technique. The random matrix can be multiplied to either left or right hand side of  $\mathbf{A}$ . We multiply the random matrix to the longer side (left side, when  $n < m$ ) of  $\mathbf{A}$ , so that the complexity of power iteration can be further reduced. Under  $m \geq n$ , the power scheme consists of  $O(mns)$  matrix multiplication and  $O(ns^2)$  QR. The polar decomposition and ED takes  $O(s^3)$ . Finally, the solution matrix composition takes  $O(mns)$ . Most expensive computations with  $O(mns)$  are simple matrix multiplications, so it can be easily parallelized.

## 3 ANALYSIS

The proposed method provides an approximate solution of SVT, thus a natural question is how accurate our algorithm is. The proposed method is analyzed by first establishing the relationship between SVT and low-rank approximation. Then, we can see, under which conditions, our method can be expected to be exact, whereby a few design tips are described in order to improve the algorithm. Besides, we show the bound comparison between our method and other representative work, Linear-Time SVD (LTSVD) [5].

### 3.1 Relationship between SVT and low-rank approximation

We can see the relationship between SVT and low-rank approximation by comparing the low-rank approximation gap and SVT operation gap for two different matrices. For ease of derivation, we slightly abuse notations, such as  $\mathbb{S}_\tau(\cdot)$  as SVT or any proximal operator and  $\mathbb{P}_\tau(\cdot)$  as corresponding dual operator of  $\mathbb{S}_\tau(\cdot)$ . We begin with reviewing useful bounds that hold for all the proximal operators, called *pseudo-contraction*<sup>3</sup> [33]:

**Proposition 2 (Pseudo-contraction [33]).** *Let  $\mathbf{A}, \mathbf{B} \in \mathbb{R}^{m \times n}$  and  $\mathbb{S}_\tau(\cdot)$  be a proximal operator. Then, the following pseudo-contraction is satisfied.*

$$\begin{aligned} & \|\mathbb{S}_\tau(\mathbf{A}) - \mathbb{S}_\tau(\mathbf{B})\|_F^2 \\ & \leq \|\mathbf{A} - \mathbf{B}\|_F^2 - \|(\mathbb{S}_\tau(\mathbf{A}) - \mathbf{A}) - (\mathbb{S}_\tau(\mathbf{B}) - \mathbf{B})\|_F^2. \end{aligned}$$

Since all the proximal operators have their corresponding dual operators, we can derive the following dual relationship based on Proposition 2.

**Corollary 1 (Dual pseudo-contraction).** *Let  $\mathbb{P}_\tau(\cdot)$  is a dual operator of  $\mathbb{S}_\tau(\cdot)$ , such that  $\mathbf{X} = \mathbb{S}_\tau(\mathbf{X}) + \mathbb{P}_\tau(\mathbf{X})$ . Then,*

$$\|\mathbb{S}_\tau(\mathbf{A}) - \mathbb{S}_\tau(\mathbf{B})\|_F^2 \leq \|\mathbf{A} - \mathbf{B}\|_F^2 - \|\mathbb{P}_\tau(\mathbf{A}) - \mathbb{P}_\tau(\mathbf{B})\|_F^2.$$

*Proof.* By using the equation  $\mathbf{X} = \mathbb{S}_\tau(\mathbf{X}) + \mathbb{P}_\tau(\mathbf{X})$ , the proof is straightforward based on Proposition 2. Thus, we omit the details.  $\square$

From here, let  $\mathbb{S}_\tau(\cdot)$  be SVT, then the dual relationship is valid by the following 2-norm ball euclidean projection operator [2].

**Definition 3 (2-norm ball euclidean projection).** *For  $\tau \geq 0$ , consider SVD of  $\mathbf{Y} = \mathbf{U}_Y \Sigma_Y \mathbf{V}_Y^\top$ . Then the 2-norm ball euclidean projection operator is defined by*

$$\mathbb{P}_\tau(\mathbf{Y}) = \mathbf{U}_Y \mathcal{P}_\tau(\mathbf{D}_Y) \mathbf{V}_Y^\top,$$

where  $\mathcal{P}_\tau(x) = \min(x, \tau)$  is an element-wise operation.

Given the 2-norm ball euclidean projection operator, we have the following lemma.

**Lemma 1.** *The 2-norm ball euclidean projection operator is the closed-form optimal solution of the following problem:*

$$\mathbb{P}_\tau(\mathbf{Y}) = \min_{\|\mathbf{X}\|_2 \leq \tau} \|\mathbf{Y} - \mathbf{X}\|_F^2.$$

*Proof.* Since the proof is straightforward, we instead provide the idea of the proof. By von Neumann's inequality, the optimal solution of  $\mathbf{X}$  should have the same singular vectors with  $\mathbf{Y}$ . Since the  $l_2$ -norm and the Frobenius norm are both unitary invariant, the problem is reduced to the diagonal matrix form. Thus, the projection operator has an explicit form as shown in Definition 3.  $\square$

The projection operator can be alternatively regarded as a proximal operator that satisfies the following corollary.

**Corollary 2.** *The euclidean projection operator  $\mathbb{P}_\tau(\cdot)$  is a proximal operator that satisfies the pseudo-contraction in Proposition 2.*

*Proof.* The first statement is valid by definition. The pseudo-contraction inequality for  $\mathbb{P}_\tau(\cdot)$  can be easily derived by replacing  $\mathbb{S}_\tau(\mathbf{X})$  to  $\mathbf{X} - \mathbb{P}_\tau(\mathbf{X})$  in the left side of Corollary 1.  $\square$

3. Refer to Lemma 3.3 of Pierra *et al.* [33]

Until now, we list basic relationships of proximal operations and their dual operations. Using them, now we can analyze the behavior of the proposed algorithm. To see this, it is meaningful to figure out the approximation error bound. Other than the randomization step in sampling  $\mathbf{Y}$ , our method is based on exact algorithms. Thus, the accuracy is only affected by the randomized range estimation, which computes a rank- $k$  approximation of a matrix. Since there is only one approximation step, the proposed method shares the same theorems with Halko *et al.* [11] as:

**Theorem 1 (Average Frobenius<sup>4</sup> error bounds by randomization [11]).** Let  $\hat{\mathbf{A}}_k$  be a rank- $k$  approximation matrix  $\mathbf{A} \in \mathbb{R}^{m \times n}$ . For a target rank  $k \geq 2$  and an over-sampling parameter  $p \geq 2$ , where  $k + p \leq \min(m, n)$ , draw an standard Gaussian matrix  $\mathbf{\Omega} \in \mathbb{R}^{n \times (k+p)}$ . Then, the theoretical minimum error and the upper bound satisfy

$$\sum_{j>k} \sigma_j^2(\mathbf{A}) \leq \mathbb{E} \|\mathbf{A} - \hat{\mathbf{A}}_k\|_F^2 \leq \text{poly}(\mathbf{v}) \cdot \sum_{j>k} \sigma_j^2(\mathbf{A}),$$

where  $\mathbb{E}$  denotes expectation with respect to the random matrix,  $\text{poly}(\mathbf{v})$  is a function for  $\mathbf{v} = \{k, p\}$  without the power iteration or  $\mathbf{v} = \{k, p, \eta\}$  with the power iteration.

For easy derivation, we only provide the squared versions for the bounds (square of the Frobenius norm). The original error bound (the Frobenius norm) can be obtained by taking the square root. Halko *et al.* show that the upper bound of the error is close to the theoretical minimum error with high probability in conjunction with some improving techniques (e.g., over-sampling and power iteration), and the bound is pessimistic.

The approximation bound of our algorithm can be obtained by connecting the low-rank approximation gap in Theorem 1 and SVT operation gap between the original and low-rank approximate matrices. We first show a steppingstone from a dual operation gap in the following.

**Proposition 3.** Let  $\hat{\mathbf{A}}_k$  be a rank- $k$  approximation of  $\mathbf{A}$ .

$$\min \|\mathbb{P}_\tau(\mathbf{A}) - \mathbb{P}_\tau(\hat{\mathbf{A}}_k)\|_F^2 = \sum_{j>k} \min(\sigma_j(\mathbf{A}), \tau)^2.$$

*Proof.* Let  $\hat{\mathbf{A}}_k = \mathbf{Q}\mathbf{Q}^* \mathbf{A} = \mathbf{P}_\mathbf{Q} \mathbf{A}$ , where  $\mathbf{Q} \in \mathbb{R}^{m \times k}$  consists of  $k$  dominant orthonormal bases, and  $\text{Range}(\mathbf{Q}) \simeq \text{Range}(\mathbf{A}_k)$  ( $\mathbf{A}_k$  is the unique and exact rank- $k$  truncated matrix of  $\mathbf{A}$ ), and  $\mathbf{P}_\mathbf{Q} = \mathbf{Q}\mathbf{Q}^*$  is an orthogonal projector. Then,

$$\begin{aligned} & \|\mathbb{P}_\tau(\mathbf{A}) - \mathbb{P}_\tau(\hat{\mathbf{A}}_k)\|_F^2 \\ &= \|\mathbb{P}_\tau(\mathbf{A}) - \mathbb{P}_\tau(\mathbf{P}_\mathbf{Q} \mathbf{A})\|_F^2 \\ &= \|\mathbb{P}_\tau(\mathbf{U}_\mathbf{A} \mathbf{\Sigma}_\mathbf{A} \mathbf{V}_\mathbf{A}^\top) - \mathbb{P}_\tau(\mathbf{P}_\mathbf{Q} \mathbf{U}_\mathbf{A} \mathbf{\Sigma}_\mathbf{A} \mathbf{V}_\mathbf{A}^\top)\|_F^2 \\ &= \|\mathbf{U}_\mathbf{A} \mathbb{P}_\tau(\mathbf{\Sigma}_\mathbf{A}) \mathbf{V}_\mathbf{A}^\top - \mathbf{P}_\mathbf{Q} \mathbf{U}_\mathbf{A} \mathbb{P}_\tau(\mathbf{\Sigma}_\mathbf{A}) \mathbf{V}_\mathbf{A}^\top\|_F^2 \\ & \quad (\text{by the property of the unitary transform}) \\ &= \|\mathbf{U}_\mathbf{A} \mathbb{P}_\tau(\mathbf{\Sigma}_\mathbf{A}) - \mathbf{P}_\mathbf{Q} \mathbf{U}_\mathbf{A} \mathbb{P}_\tau(\mathbf{\Sigma}_\mathbf{A})\|_F^2 \\ & \quad (\text{by the unitary invariant of the norm}) \\ &= \|(\mathbf{I} - \mathbf{P}_\mathbf{Q}) \mathbf{U}_\mathbf{A} \mathbb{P}_\tau(\mathbf{\Sigma}_\mathbf{A})\|_F^2 \\ &= \|\mathbf{P}_\mathbf{Q}^\perp \mathbf{U}_\mathbf{A} \mathbb{P}_\tau(\mathbf{\Sigma}_\mathbf{A})\|_F^2. \end{aligned}$$

$\mathbf{P}_\mathbf{Q}^\perp = \mathbf{I} - \mathbf{P}_\mathbf{Q}$  is the orthogonal projector onto the complementary subspace  $\text{Range}(\mathbf{P}_\mathbf{Q})^\perp$ , which is also close to  $\text{Range}(\mathbf{A}_k)^\perp$ . Thus, the minimum is achieved only when

4. For easy derivation, we provide the squared versions (the square of the Frobenius norm) for Theorems 1 and 2. The original error bound (the Frobenius norm) can be obtained by taking the square root.

$\text{Range}(\mathbf{P}_\mathbf{Q}) = \text{Range}(\mathbf{A}_k)$  or  $\text{Range}(\mathbf{P}_\mathbf{Q})^\perp = \text{Range}(\mathbf{A}_k)^\perp$ . Then,

$$\min \|\mathbf{P}_\mathbf{Q}^\perp \mathbf{U}_\mathbf{A} \mathbb{P}_\tau(\mathbf{\Sigma}_\mathbf{A})\|_F^2 = \sum_{j>k} \min(\sigma_j(\mathbf{A}), \tau)^2. \quad \square$$

From Theorem 1 and Proposition 3, the following theorem is our main result for the bound of the approximate SVT.

**Theorem 2 (Average error bound of the approximate SVT).** Let  $\mathbb{S}_\tau(\cdot)$  be the SVT operator. The average error satisfies the following inequality.

$$\mathbb{E} \|\mathbb{S}_\tau(\mathbf{A}) - \mathbb{S}_\tau(\hat{\mathbf{A}}_k)\|_F^2 \leq \text{poly}(\mathbf{v}) \cdot \left( \sum_{j>k} \sigma_j^2(\mathbf{A}) \right) - G(\mathbf{A}),$$

where  $G(\mathbf{A}) = \sum_{j>k} \min(\sigma_j(\mathbf{A}), \tau)^2 \geq 0$ .

*Proof.* By Corollary 1, 2 and Proposition 3,

$$\begin{aligned} \|\mathbb{S}_\tau(\mathbf{A}) - \mathbb{S}_\tau(\hat{\mathbf{A}}_k)\|_F^2 &\leq \|\mathbf{A} - \hat{\mathbf{A}}_k\|_F^2 - \|\mathbb{P}_\tau(\mathbf{A}) - \mathbb{P}_\tau(\hat{\mathbf{A}}_k)\|_F^2 \\ &\leq \|\mathbf{A} - \hat{\mathbf{A}}_k\|_F^2 - \sum_{j>k} \min(\sigma_j(\mathbf{A}), \tau)^2. \end{aligned}$$

Take the expectation to the both sides,

$$\begin{aligned} & \mathbb{E} \|\mathbb{S}_\tau(\mathbf{A}) - \mathbb{S}_\tau(\hat{\mathbf{A}}_k)\|_F^2 \\ &\leq \mathbb{E} \|\mathbf{A} - \hat{\mathbf{A}}_k\|_F^2 - \sum_{j>k} \min(\sigma_j(\mathbf{A}), \tau)^2 \\ &\leq \text{poly}(\mathbf{v}) \cdot \left( \sum_{j>k} \sigma_j^2(\mathbf{A}) \right) - \sum_{j>k} \min(\sigma_j(\mathbf{A}), \tau)^2, \\ & \quad (\text{by Theorem 1}) \\ &= \text{poly}(\mathbf{v}) \cdot \left( \sum_{j>k} \sigma_j^2(\mathbf{A}) \right) - G(\mathbf{A}) \end{aligned}$$

Obviously,  $G(\mathbf{A}) \geq 0$  by the definition.  $\square$

Comparing the right hand side bounds from Theorems 1 and 2, since  $G(\mathbf{A}) \geq 0$ , the bound of Theorem 2 is smaller than the one of Theorems 1.

In Theorems 1 and 2, in the case without power iteration,  $\text{poly}(\cdot)$  is defined as:

$$\text{poly}(\mathbf{v} = \{k, p\}) = (1 + k/(p-1)). \quad (8)$$

The polynomial bound with power iteration with the Frobenius norm representation has no simple form [11], so instead we observe the error bound with power iteration by referring to the spectral bound in the following Theorem 3 and Corollary 3.

**Theorem 3 (Average spectral error bound by randomization with the power scheme [11]).** Let  $\eta$  be the number of power iterations,  $l = k + p$  be a sampling rate. Then, the theoretical minimum error and upper bound satisfy

$$\begin{aligned} \sigma_{k+1} &\leq \mathbb{E} \|\mathbf{A} - \hat{\mathbf{A}}_k\|_2 \leq \\ & \left[ \left( 1 + \sqrt{\frac{k}{p-1}} \right) \sigma_{k+1}^{2\eta+1} + \frac{e\sqrt{k+p}}{p} \left( \sum_{j>k} \sigma_j^{2(2\eta+1)} \right)^{\frac{1}{2}} \right]^{\frac{1}{2\eta+1}}, \end{aligned} \quad (9)$$

where  $\sigma_i = \sigma_i(\mathbf{A})$ .

**Corollary 3** ([11]). Theorem 3 is bounded as

$$\mathbb{E} \|\mathbf{A} - \hat{\mathbf{A}}_k\|_2 \leq \text{poly}(\mathbf{v}) \cdot \sigma_{k+1}, \quad (10)$$

where  $\text{poly}(\mathbf{v}) = \left[ 1 + \sqrt{\frac{k}{p-1}} + \frac{e\sqrt{k+p}}{p} \cdot \sqrt{h-k} \right]^{\frac{1}{2\eta+1}}$ ,  $\mathbf{v} = \{k, p, \eta\}$ , and  $h = \min(m, n)$ .

Corollary 3 is only useful for understanding the bound behavior of the power scheme rather than a tight bound, because it is far broader than Theorem 3. However, it shows that, as  $\eta$  increases,  $\text{poly}(\mathbf{v})$  approaches 1 exponentially fast, and when  $\text{poly}(\mathbf{v}) \sim 1$ , the spectral error is bounded by the theoretical minimum  $\sigma_{k+1}$ . Our bound also follows the same behavior.

Consequently, our Theorem 2 asserts that the bound of approximate SVT is tighter than the error by rank- $k$  approximation in Theorem 1 on average. Thus, in practice, we have the following properties from Theorem 2:

- Once  $\sigma_{k+1}(\mathbf{A})$  approach to a small value, then  $\|\mathbb{S}_\tau(\mathbf{A}) - \mathbb{S}_\tau(\hat{\mathbf{A}}_k)\|_F^2$  may approach to close to zero, *i.e.*, which means almost exact roughly when  $k \geq \text{rank}(\mathbf{A})$ . Detail analyses on how small value for  $\sigma_{k+1}(\mathbf{A})$  and a milder condition for exactness are derived in Sec. 3.2.
- Fortunately, the bound becomes rapidly tighter as  $p$  or  $\eta$  increases in both practice and theory, similar to the result of Halko *et al.* [11].
- The bound is independent of the matrix size.

### 3.2 Exactness

Though in the previous section, we state that our algorithm produces almost exact results when  $k \geq \text{rank}(\mathbf{A})$ , we may have a broader condition for the exactness because the bound in Theorem 2 is tighter than that of low-rank approximation in Theorem 1. In this section, we investigate conditions in which the proposed method can be expected to be exact rather than approximate. We have the following result.

**Proposition 4.** Let  $\text{poly}(\mathbf{v}) = \left(1 + \frac{k}{p-1}\right)$  (the case without power iteration). Then, FRSVT can be expected to be exact, for matrix  $\mathbf{A}$  satisfying

$$\sigma_{k+1}(\mathbf{A}) \leq \frac{\tau}{\sqrt{1 + \frac{k}{p-1}}}. \quad (11)$$

*Proof.* From Theorem 2, we rewrite the right bound as:

$$\begin{aligned} & \text{poly}(\mathbf{v}) \cdot \sum_{j>k} \sigma_j^2(\mathbf{A}) - \sum_{j>k} \min(\sigma_j(\mathbf{A}), \tau)^2 \\ &= \left(1 + \frac{k}{p-1}\right) \sum_{j>k} \sigma_j^2(\mathbf{A}) + \sum_{j>k} \max(-\sigma_j(\mathbf{A})^2, -\tau^2) \\ &= \frac{k}{p-1} \sum_{j>k} \sigma_j^2(\mathbf{A}) + \sum_{j>k} \max(0, \sigma_j(\mathbf{A})^2 - \tau^2) \\ &= \sum_{j>k} \max\left(0, \left(1 + \frac{k}{p-1}\right) \sigma_j^2(\mathbf{A}) - \tau^2\right). \end{aligned}$$

Since  $\left(1 + \frac{k}{p-1}\right)$  and  $\tau$  are constant, and  $\sigma_j^2(\mathbf{A}) \leq \sigma_{j+1}^2(\mathbf{A})$ , if  $\left(1 + \frac{k}{p-1}\right) \sigma_{k+1}^2(\mathbf{A}) - \tau^2 \leq 0$ , the upper bound of Theorem 2 becomes zero, *i.e.*, exact. Therefore, when  $\sigma_{k+1}(\mathbf{A}) \leq \frac{\tau}{\sqrt{1 + \frac{k}{p-1}}}$ , the proposed FRSVT can be expected to be exact.  $\square$

For simplicity, we have only considered the case without power iteration, but from Corollary 3, we can deduce that  $\text{poly}(\mathbf{v})$  with power iteration would be smaller than  $\left(1 + \frac{k}{p-1}\right)^5$ . This makes the bound condition in Eq. (11) broader with power iteration. The presented analysis provides

5. Halko *et al.* [11] show that the power iteration scheme significantly improves the approximation bound quality, and the bound is tighten exponentially fast as increasing  $\eta$  in  $\mathbf{v}$ .

a few design tips for an efficient implementation of the FRSVT algorithm.

**Design Tips** The bound obtained in Proposition 4 can be used to determine whether to use power iteration (or how to set  $\eta$  in  $\mathbf{v}$ ) in each iteration or to design a better rank prediction rule in Sec. 2.3. Specifically, after the range propagation step, given  $\mathbf{Q}$ , we compute  $\mathbf{B} = \mathbf{Q}^\top \mathbf{A} \in \mathbb{R}^{s \times n}$ , which is typically a fat matrix. Then, the smallest eigen value  $\sigma_s^2(\hat{\mathbf{A}})$  can be efficiently estimated from a small positive semi-definite matrix  $\mathbf{B}\mathbf{B}^\top$ . By checking the bound condition in Eq. (11), we can determine the necessity of power iteration or the value of  $\eta$  in that iteration.

Additional to checking singular values at each iteration, we can check the value of the soft threshold  $\tau$  as in Eq. (11) in order to reduce computational waste. By checking it, we can decide elaborately whether to use additional treatments such as the number of the power iteration or large over-sampling. Since  $\tau$  is typically set to large in early iterations of NNM related optimizations, FRSVT may result in reasonable accuracy even without special treatment. In later iterations of the optimization,  $\tau$  would be getting smaller for fine tuning of optimization variables. Then, by increasing over-sampling rate  $p$ , applying power iteration or adjusting  $\eta$ , we could maintain rational accuracy with reducing unnecessary computation burden.

### 3.3 Bound Comparison with Linear-Time SVD

We show the error bound comparison with a relevant method by showing the approximation error bound of Drineas *et al.* [5].

**Theorem 4 (Average error bound of LTSVD [5]).** Let  $\mathbf{A} \in \mathbb{R}^{m \times n}$  and  $\mathbf{H}_k$  be a matrix created by the LINEAR-TIMESVD algorithm [5] by sampling  $c$  columns of  $\mathbf{A}$  with probabilities  $\{p_i\}_{i=1}^n$  such that  $p_i \geq \beta |\mathbf{A}^{(i)}|^2 / \|\mathbf{A}\|_F^2$  for some positive  $\beta \leq 1$  and  $\epsilon > 0$ . If  $c \geq 4k/\beta\epsilon^2$ , then the average Frobenius error is bounded by

$$\mathbb{E}\|\mathbf{A} - \mathbf{H}_k \mathbf{H}_k^\top \mathbf{A}\|_F^2 = \mathbb{E}\|\mathbf{A} - \hat{\mathbf{A}}_k\|_F^2 \leq \|\mathbf{A} - \mathbf{A}_k\|_F^2 + \epsilon \|\mathbf{A}\|_F^2.$$

In addition, the average spectral error is bounded by

$$\mathbb{E}\|\mathbf{A} - \mathbf{H}_k \mathbf{H}_k^\top \mathbf{A}\|_2 = \mathbb{E}\|\mathbf{A} - \hat{\mathbf{A}}_k\|_2 \leq \sqrt{\|\mathbf{A} - \mathbf{A}_k\|_2^2 + \epsilon \|\mathbf{A}\|_F^2}.$$

For a fair comparison, we set same parameters when comparing the low-rank approximation bounds of Drineas *et al.* and Halko *et al.* [11], *i.e.*, the over-sampling rate to be same as the specified target rank  $k$ .

**Corollary 4.** Suppose that the sampling rate  $c$  is set to two times larger than the target rank  $k$ , *i.e.*,  $c = 2k$ , then

$$\epsilon \geq \sqrt{2}.$$

and LTSVD also holds the following bounds:

$$\mathbb{E}\|\mathbf{A} - \hat{\mathbf{A}}_k\|_F^2 \leq \sum_{j>k} \sigma_j^2(\mathbf{A}) + \sqrt{2} \sum_{j=1}^{\min(m,n)} \sigma_j^2(\mathbf{A}), \quad (12)$$

$$\mathbb{E}\|\mathbf{A} - \hat{\mathbf{A}}_k\|_2 \leq \left( \sigma_{k+1}^2(\mathbf{A}) + \sqrt{2} \sum_{j=1}^{\min(m,n)} \sigma_j^2(\mathbf{A}) \right)^{\frac{1}{2}}. \quad (13)$$

*Proof.* From Theorem 4, we have  $\beta \leq 1$ ,  $\epsilon > 0$  and  $c \geq 4k/\beta\epsilon^2$ . Therefore,

$$\epsilon \geq 2\sqrt{\frac{k}{\beta c}}.$$

Since the lowest bound can be achieved at  $\beta = 1$ , and  $c = 2k$  is assumed,

$$\epsilon \geq 2\sqrt{\frac{k}{c}} = \sqrt{2}.$$

In addition, we can obtain Eq. (12) and Eq. (13) from the following bounds by setting the above result to Theorem 4.

$$\mathbb{E}\|\mathbf{A} - \hat{\mathbf{A}}_k\|_F^2 \leq \|\mathbf{A} - \mathbf{A}_k\|_F^2 + \sqrt{2}\|\mathbf{A}\|_F^2.$$

The average spectral bound can be also derived analogously.  $\square$

From Corollary 4 and Theorem 1, we obtain the following conclusion.

**Proposition 5.** *Suppose the target rank  $k \geq 4$  and the over-sampling rate to be  $k$  (for Halko et al. [11],  $p = k$ , and for LTSVD,  $c = 2k$ ), then on average Halko et al. [11] without power iteration has a tighter bound than LTSVD.*

*Proof.* We compare the right bound terms of Theorem 1 and Corollary 4 in Eq. (12).

$$[\text{LTSVD}] \quad \sum_{j>k} \sigma_j^2(\mathbf{A}) + \sqrt{2} \sum_{j=1}^{\min(m,n)} \sigma_j^2(\mathbf{A}). \quad (14)$$

$$[\text{Halko et al.}] \quad \text{poly}(\mathbf{v}) \cdot \sum_{j>k} \sigma_j^2(\mathbf{A}). \quad (15)$$

Suppose that Eq. (14) < Eq. (15).

$$\begin{aligned} & \sum_{j>k} \sigma_j^2(\mathbf{A}) + \sqrt{2} \sum_{j=1}^{\min(m,n)} \sigma_j^2(\mathbf{A}) < \text{poly}(\mathbf{v}) \cdot \sum_{j>k} \sigma_j^2(\mathbf{A}) \\ \Rightarrow & -\frac{k}{k-1} \sum_{j>k} \sigma_j^2(\mathbf{A}) + \sqrt{2} \sum_{j=1}^{\min(m,n)} \sigma_j^2(\mathbf{A}) < 0 \\ \Rightarrow & \sqrt{2} \sum_{1 \leq j \leq k} \sigma_j^2(\mathbf{A}) + C(k) \cdot \sum_{j>k} \sigma_j^2(\mathbf{A}) < 0 \quad (16) \\ & \left( C(k) = \sqrt{2} - \frac{k}{k-1} \right) \end{aligned}$$

For  $k \geq 4$ , the minimum of  $C(k)$  is achieved at  $k = 4$  as  $C(4) = \sqrt{2} - \frac{4}{3} > 0$ . Thus, since  $C(k) > 0$  for  $k \geq 4$ , the left term of Eq. (16) is positive for  $k \geq 4$ . This contradicts the assumption that Eq. (14) < Eq. (15), which concludes the proof.  $\square$

For simplicity, we make a reasonable assumption, the target rank  $k \geq 4$ . Since the bound comparison is done without the power iteration scheme, Halko et al. may have a loose bound. However, as shown in Proposition 5, Halko et al. still results in better approximation bound than LTSVD even under handicapped condition (i.e., sampling rate). Companionship with the power iteration, one could derive broader conditions that Halko et al. perform better than LTSVD by similarly following the proof process of Proposition 5.

## 4 EXPERIMENTAL RESULTS

In this section, we first evaluate the efficiency of the proposed method in comparison with other methods using simulation data. The evaluation is conducted by examining the performance of a single SVT computation and also by RPCA computation, which is arguably the most relevant NNM problem in computer vision today. We then show NNM applications in computer vision using real-world data; subspace clustering,

SVD <sub>Matlab 2010a</sub>	Built-in SVD(, 'econ') is based on Intel MKL 10.2.2 and LAPACK 3.2.1.
SVD <sub>Matlab 2014a</sub>	Built-in SVD(, 'econ') is based on LAPACK 3.4.1 in Intel MKL 11.0.5.
LTSVD*	The Matlab implementation by Ma et al. [25] is used.
Lanczos	The implementation optimized by Lin et al. [16] is used. It is implemented by Matlab and Mex to use LAPACK (ver. 3.4.1 in Intel MKL 11.0.5 is used).
BLWS	The Matlab implementation by Lin et al. [19] is used.
Mu et al.	The Matlab implementation provided by Mu et al. [27] is used. All the parameters are directly used as suggested.
FSVT***	We implement FSVT by Matlab and Mex based on Intel MKL 11.0.5, and the speed-up gain is checked and consistent with the reported results in Cai et al. [2]. All the parameters are directly used as suggested.
RSVD***	We implement RSVD [11] based on LAPACK 3.4.1 in Intel MKL 11.0.5. by referring to RedSVD**.
FRSVT***	Our Matlab implementation based on Intel MKL 11.0.5. Partially, we implement Mex functions for QR-CP (dgeqp3) and Polar Decomposition with BLAS and LAPACK 3.4.1 routines.

\* LTSVD: In the implementation of [25], the leverage score estimation suggested by the original paper [5] is omitted, which is required for the importance sampling. So we implement it with  $O(mn)$  complexity.

\*\* RedSVD (<http://code.google.com/p/reedsvd/>): Since RedSVD is implemented based on Eigen 3.0-b1, without the power iteration, so the original implementation is not fast and inaccurate. Thus, we re-implement RSVD [11] by just referring to RedSVD (2-sides random projection).

\*\*\* For FSVT, RSVD and FRFSVT implementation, we utilize Armadillo library [34] as a high level wrapper for LAPACK and BLAS of Intel MKL in our Mex implementation part. In the Mex functions of Lanczos, Lin et al. [16] directly call LAPACK routines without any external library.

TABLE 2: Lists of comparison methods and details for SVT tests. All the parallelization techniques are turned off for fair comparison.

semi-online weather artifact removal, and simultaneous multi-image alignment and rectification. All the experiments are conducted on a PC with Intel i7-3.4GHz and 16GB RAM. The same shared parameters were used among different algorithms.

### 4.1 Evaluation using Simulation Data

We quantitatively evaluate our method in comparison to other methods with synthetic matrices sampled from a standard Gaussian distribution. Computational times are evaluated using Matlab 2010a and 2014a 64bits. Since the recent Matlab has been intensively optimized on Intel CPU (mainly due to improvement of Intel MKL), the computation efficiency has been noticeably improved. Therefore, it is worth reporting the performance difference on these two versions of Matlab, because most related works have been assessed with Matlab older than 2011a [2], [19], [21], [22], [27]. For a fair comparison, we turn off multi-threading functions including `maxNumCompThreads(1)` in Matlab. We describe the implementation details of each method in Table 2.

**Single SVT test** Figure 4 compares speed and accuracy of SVT computation using SVT methods, such as Matlab built-in SVD<sup>6</sup> (baseline), Lanczos [16], FSVT [2], LTSVD [5] and our FRFSVT (with / without RP). All the implementation details are

6. We apply either the economic size or full SVD depending on the matrix shape and report the faster one, but we denote either as econSVD.

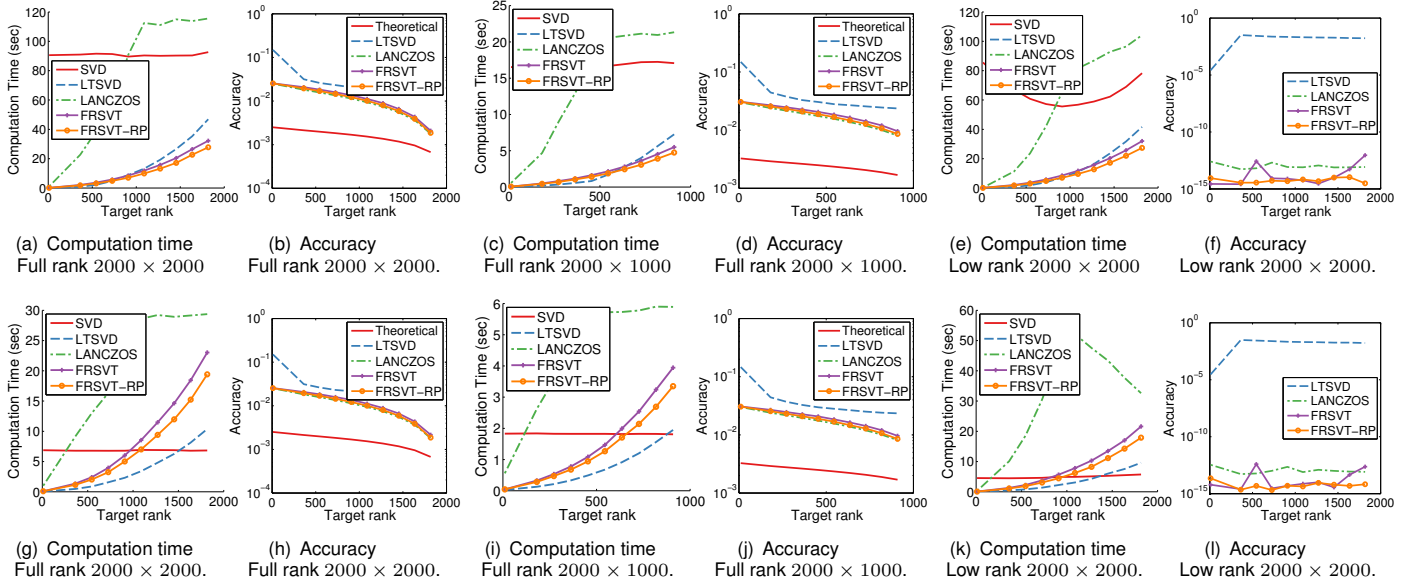


Fig. 4: SVT comparisons among SVD methods. [Top] Experiments on Matlab 2010a. [Bottom] Experiments on Matlab 2014a. Accuracy is measured by normalized root mean squared error (NRMSE),  $\|\mathbf{A}^* - \hat{\mathbf{A}}_k\|_F / \|\mathbf{A}^*\|_F$ , where  $\mathbf{A}^* = \mathbb{S}_\tau(\mathbf{D}_{GT})$ ,  $\hat{\mathbf{A}}_k = \mathbb{S}_\tau(\mathbf{D}_k)$ ,  $\mathbf{D}_{GT}$  is the input data, and  $\mathbf{D}_k$  is approximated by each method. For the low-rank matrix test, we generate input data matrices whose rank correspond to the target rank by multiplying two Gaussian random matrices with  $m \times r$  and  $r \times n$ , while in other tests full rank matrices are used. In (b,d,h,j), the theoretical minimum error bound by rank truncation in  $\mathbb{S}_\tau(\mathbf{D}_k)$  is provided for guidance, and it is defined as  $\sum_{j>k} \sigma_j(\mathbf{A}^*)$ , where  $\sigma_i(\mathbf{A}^*)$  is computed by Matlab built-in SVD. For the low-rank case in (f,i), the theoretical minimum error is zero, so we omit the theoretical bound.

Methods	$p$	AP	PI
iALM <sub>econSVD</sub>	-	×	-
iALM <sub>LTSVD</sub>	+5	○	-
iALM <sub>BLWS</sub>	-	○	-
Mu <i>et al.</i> [27]	-	×	-
iALM <sub>FSVT</sub>	-	×	-
iALM <sub>RSVD</sub>	+5	○	2
iALM <sub>FRSVT</sub>	+2	○	2
iALM <sub>FRSVT-RP</sub>	+2	○	2

TABLE 3: Parameter settings for convergence evaluation of RPCA. ( $p$ : Over-sampling rate, AP: Adaptive rank prediction, PI: The number of power iterations  $\eta$ .)

summarized in Table 2. Except for the baseline SVD, the others produce the truncated SVD of the input matrix, and it is used for SVT computation.

We test using Gaussian random matrix drawn from  $N(0, 1)$  for the operation  $\mathbb{S}_\tau[\cdot]$  with  $\tau = 1/\sqrt{\|\mathbf{A}\|_2}$ . For a rank- $k$  approximation, we compute rank- $(k + p)$  approximations by setting the over-sampling rate  $p$  to 2 for Lanczos,  $k$  for LTSVD, 5 for FRSVT. We apply the power iteration twice, *i.e.*,  $q = 2$ . While LTSVD in Fig. 4(e) is faster than ours, the approximation error is significantly higher than other truncated SVDs, and it results in slower convergence in RPCA as we will see in the following. We explain theoretical comparison between LTSVD and FRSVT in Proposition 5.

**Robust PCA test** To observe the convergence behavior of SVT methods in RPCA [3], we compare our method with various SVT methods, such as SVD, LTSVD, BLWS [19], FSVT, RSVD [11], using an inexact augmented Lagrange multiplier method [17] (iALM, or called alternating directional multiplier method)<sup>7</sup> in Figs. 5 and 6 for continuous behaviors, and Table 4 for resultant performance. We set the trade-off parameter

7. For Mu *et al.* [27], we could not reproduce their result. However, we include the results for thoroughness. The results are consistent with the early reported results in Liu *et al.* [22].

Computational Time (s)

	LRR+SVD		LRR+Ours
	Matlab 2010a	Matlab 2014a	
Time per Motion	1.230	1.016	0.452
Time for 640 Faces	419.440	75.216	44.590

TABLE 5: Comparisons of the subspace segmentation algorithms on Hopkins155 [36] (Motion) and Extended Yale Database B [15] (Face). Motion Segmentation Errors on the Hopkins155 of both LRR and LRR+Ours are 1.59%. The segmentation accuracies (%) on the Yale data are 79.06 for both LRR and LRR+Ours. These results show the improvement of the computation time with retaining the same accuracy.

$\lambda = \frac{1}{\sqrt{\max(m,n)}}$  as suggested by Candès *et al.* [3] for all the methods. All other parameters for FRSVT are same as mentioned in Sec. 2 and with Table 3. We apply the proposed adaptive rank prediction described in Sec. 2.3 to LTSVD, RSVD and our FRSVT. LTSVD shows convergence degradation to achieve comparable accuracy with others due to rough approximation on both bases and singular values. Other methods including our FRSVT show similar numbers of iterations and accuracy, but our method has a considerably lower computation time for a single iteration.

## 4.2 More Applications

We show more general applications of our FRSVT method to various types of low-rank optimization problems summarized in Table 6, such as affine constrained NNM (Type A), non-convex truncated NNM (Type B) and NNM on tensor structure (Type C). We show them with typical computer vision applications in the following.

**Type A - Robust Subspace Clustering by Low-Rank Representation (LRR)** Many visual data is often characterized by a mixture of multiple subspaces. One of the recent promising methods is LRR, which effectively performs subspace clustering and noise correction simultaneously. While both noise correction and subspace clustering are known to be challenging,

	iALM <sub>econSVD</sub>		iALM <sub>LTSVD</sub>	iALM <sub>BLWS</sub>	Mu <i>et al.</i>	iALM <sub>FSVT</sub>	iALM <sub>RSVD</sub>	iALM <sub>FRSVT-RP</sub>
	Matlab 2010a	Matlab 2014a						
	$\ S\ _0$							
10000 × 100	99,999		879,415	99,999	999,999	99,999	99,999	99,999
2000 × 2000	399,997		994,479	399,998	3,998,401	399,997	399,997	399,997
4000 × 4000	1,599,981		5,607,211	1,599,984	15,995,318	1,599,981	1,599,981	1,599,981
6000 × 6000	-	3,599,952	35,662,548	3,599,966	35,990,553	3,599,952	3,599,952	3,599,952
	Accuracy							
10000 × 100	7.34e-05		3.39e-02	2.66e-04	7.65e-01	7.34e-05	7.31e-05	9.33e-05
2000 × 2000	2.11e-07		7.77e-07	1.03e-06	1.10e+00	2.11e-07	2.11e-07	2.11e-07
4000 × 4000	1.81e-07		4.59e-07	4.83e-07	1.37e+00	1.81e-07	1.81e-07	1.81e-07
6000 × 6000	-	1.42e-07	7.76e-05	3.83e-07	1.49e+00	1.42e-07	1.43e-07	1.43e-07
	Total Time							
10000 × 100	3.217	1.982	1.722	1.317	125.368	2.436	0.970	0.782
2000 × 2000	2751.910	147.055	11.075	9.808	118.798	348.132	12.497	5.123
4000 × 4000	21668.280	1068.863	69.547	53.468	759.794	2527.141	80.705	30.274
6000 × 6000	-	3360.379	203.051	164.752	2385.272	8238.109	149.204	88.132
	Avg. time for a single iteration							
10000 × 100	0.140	0.086	0.039	0.049	1.687	0.104	0.042	0.034
2000 × 2000	119.415	6.393	0.274	0.393	1.667	15.189	0.557	0.226
4000 × 4000	947.908	46.481	1.726	2.185	10.664	110.006	3.623	1.348
6000 × 6000	-	146.192	4.295	6.848	33.505	358.899	6.681	3.942
	Total no. iteration							
10000 × 100	23		43	24	73	23	23	23
2000 × 2000	23		41	24	70	23	23	23
4000 × 4000	23		41	24	70	23	23	23
6000 × 6000	-	23	48	24	70	23	23	23
	Speed-up gain against the baseline							
10000 × 100	-	1.62 ×	1.87 ×	2.44 ×	0.03 ×	1.32 ×	3.32 ×	4.11 ×
2000 × 2000	-	18.71 ×	248.48 ×	280.58 ×	23.16 ×	7.90 ×	220.21 ×	537.17 ×
4000 × 4000	-	20.27 ×	311.56 ×	405.26 ×	28.52 ×	8.57 ×	268.49 ×	715.74 ×
6000 × 6000	-	-	-	-	-	-	-	-

TABLE 4: Quantitative comparison on RPCA. The accuracy is measured by NRMSE with the ground-truth data, and the speed-up gain is computed against the baseline method, iALM<sub>econSVD</sub> on Matlab 2010a. For Mu *et al.* [27], we used the implementation and parameters provided by the authors. Since Mu *et al.* is based on the exact ALM algorithm [17], while other methods are based on the inexact ALM [17], we report the times for a single outer iteration of Mu *et al.* as ‘Avg. time for a single iteration.’ In addition, the highly stochastic property of the randomly projected nuclear norm makes the algorithm [27] sensitive to data and does not preserve the singular values and sparsity structure of the matrix. This result is consistent with another stochastic method, LTSVD (see and compare  $\|S\|_0$  of LTSVD and Mu *et al.*).

Type	Objective function	Constraint
A	$\operatorname{argmin}_{L,S} \ L\ _* + \lambda \ S\ _{2,1}$	$O = ZL + S$
B	$\operatorname{argmin}_{L,S} \sum_{i=k+1}^n \sigma_i(L) + \lambda \ S\ _1$	$O = L + S$
C	$\operatorname{argmin}_{L,\mathcal{E},\Gamma} \sum_{i=1}^3 \alpha_i \ L_{(i)}\ _* + \lambda \ \mathcal{E}\ _1$	$O \circ \Gamma = L + \mathcal{E}$

TABLE 6: Examples of NNM related objective functions. (A) Low-rank representation. (B) RPCA based on the non-convex truncated nuclear norm, where  $k$  is the target rank. (C) Low-rank and sparse 3-order tensor decomposition with alignment. Here,  $\|\cdot\|_{2,1}$  is  $l_{2,1}$  norm,  $\{\alpha_i\}$  are balancing parameters among the unfolding matrices  $\mathcal{L}_{(i)}$ , and  $\sum \alpha_i = 1$  is assumed. We refer the basic tensor algebra notations described in [38].

robust LRR has been shown robust against large corruptions. The robust LRR can be formulated by Type A, which can be efficiently solved by iALM. In this experiment, we use the same parameter settings and evaluation metrics suggested in [20].

We apply FRSVT to the robust LRR for motion segmentation on Hopkins155 [36] and for face recognition on a part of Extended Yale Database B [15], respectively. All parameters for FRSVT are same as mentioned in Sec. 2. We use all the 156 sequences in Hopkins155, and the first 10 classes in Extended Yale Database B, in which each class contains 64 face images captured under various illumination conditions – given  $42 \times 48$  resized images, we construct a  $2016 \times 640$  data matrix by vectorizing each image. While Hopkins155 is only weakly corrupted, Yale data is heavily corrupted by shadows, specularity and noise. As shown in Table 5, our method speeds up LRR without degrading of the accuracy.

**Type B - Semi-Online Weather Artifact Removal** We consider a weather artifacts (e.g., snow or rain) removal problem in a video sequence. Since the weather artifacts have non-

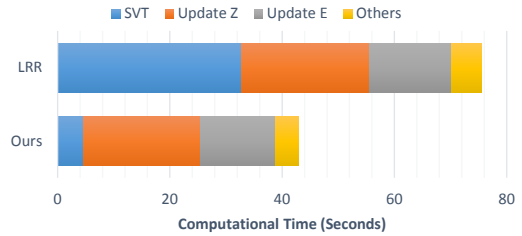


Fig. 7: Computation time comparison on the subspace clustering application [20]. Computation times are measured for face clustering on Extended Yale Database B [15].

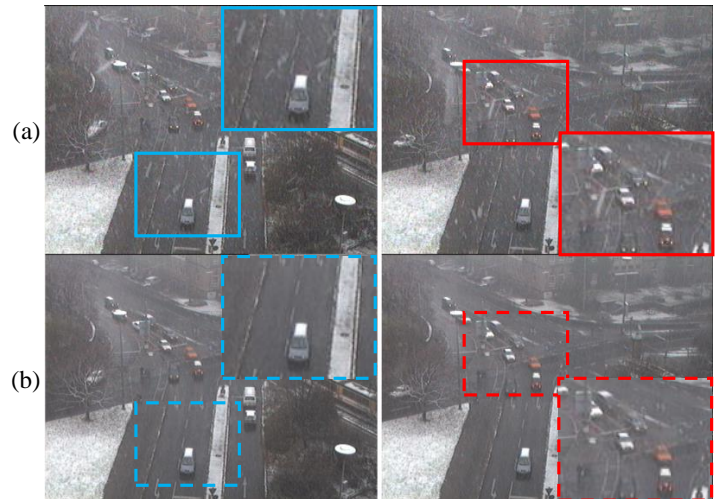


Fig. 8: Qualitative results for the weather artifact removal. (a) Sample input images O. (b) Low-rank images Z.

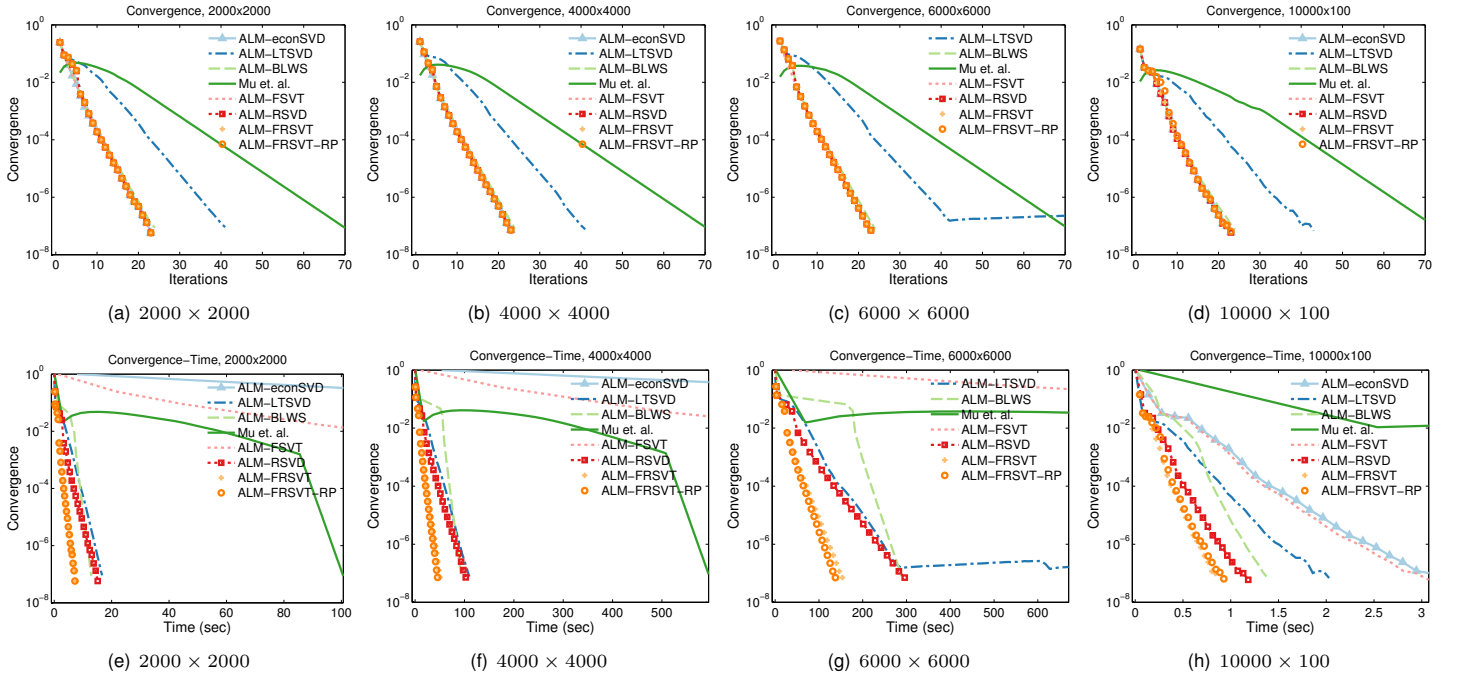


Fig. 5: RPCA comparisons on Matlab 2010a. [Top] X-axis: Number of iterations, Y-axis: Stopping criterion. [Bottom] X-axis: Elapsed time (sec.), Y-axis: Stopping criterion. Except *Mu et al.* is based on the exact ALM method, all the other methods are based on the inexact ALM.

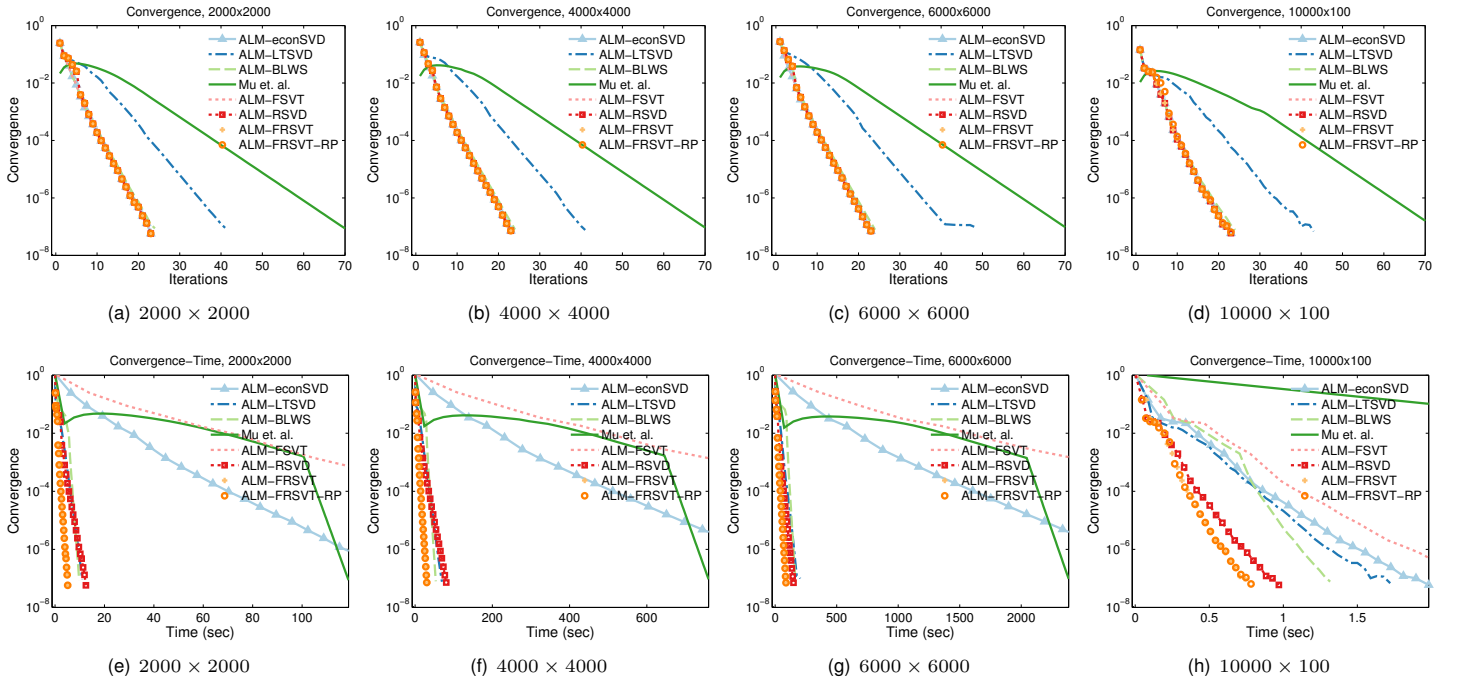


Fig. 6: RPCA comparisons on Matlab 2014a. [Top] X-axis: Number of iterations, Y-axis: Stopping criterion. [Bottom] X-axis: Elapsed time (sec.), Y-axis: Stopping criterion. Except *Mu et al.* is based on the exact ALM method, all the other methods are based on the inexact ALM.

deterministic appearance and a sparse yet random distribution in the spatio-temporal domain, we model the artifacts as sparse outlier and the scene as low-rank, while we want to retain moving objects. We apply the low-rank and sparsity decomposition to  $n$  frames in a sliding window manner to leave moving objects in the latent images.

Unfortunately, since finding low-rank solution by the nuclear norm is based on the blessing of high dimensionality [3], it could be degraded with a small number of frames as reported in *Oh et al.* [28]. With the assumption that the object motions are small within a few frames, we can encourage the low-

rank solution to be rank-1 and decompose sparse corruptions by Type B optimization with  $k = 1$ , where  $\mathbf{O}$  is constructed by stacking vectorized  $n$  images. It can be effectively solved by alternating Partial SVT (PSVT) [28] and  $l_1$  minimization based on iALM. We replace PSVT by FRSVT with the partial thresholding. We transfer the previous basis estimation to the next  $n$  frame optimization, so it can be regarded as a semi-online algorithm.

We set the trade-off parameter  $\lambda = \frac{1}{\sqrt{\max(m,n)}}$  as suggested by *Oh et al.* [28], and limit the maximum rank- $l$  for computing

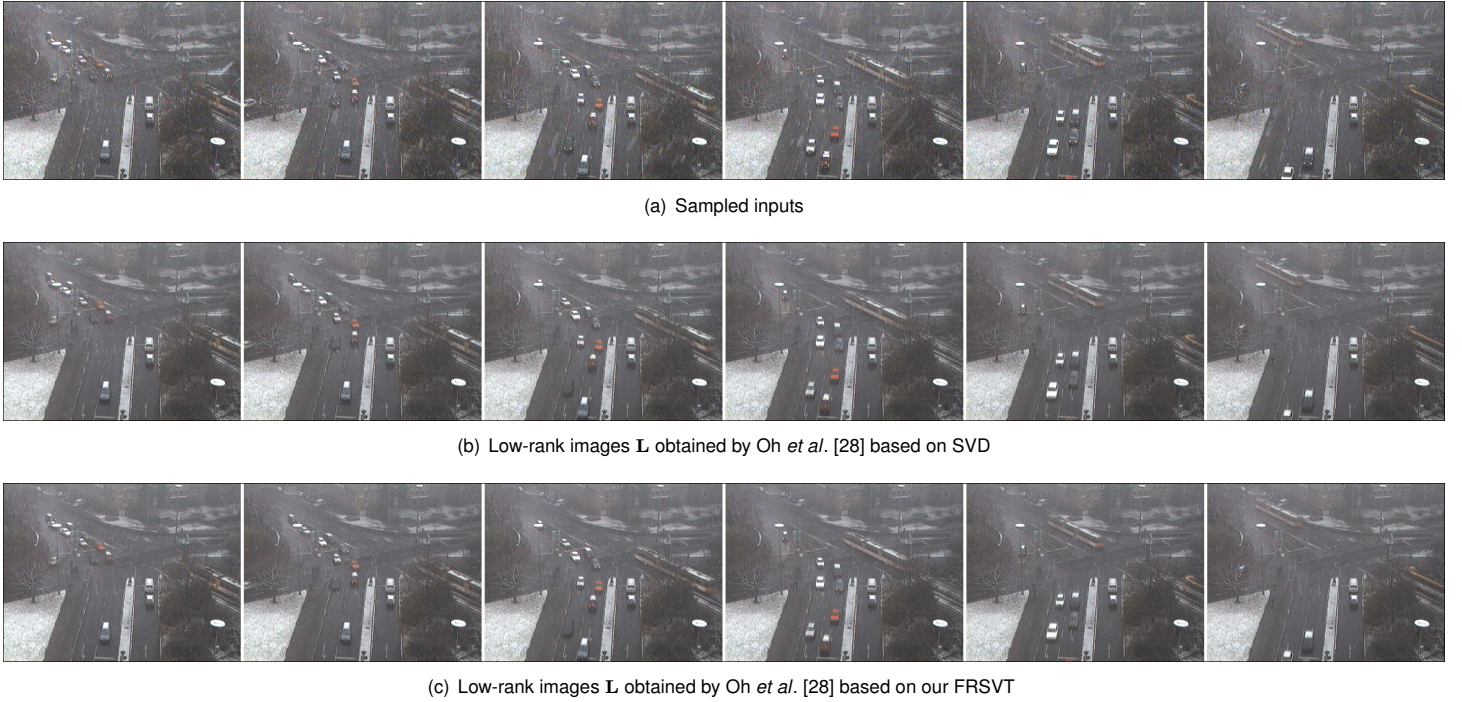


Fig. 9: Sampled results for the weather artifact removal with the sliding window length 5.

	Computational Time (ms)			
Sliding Window $n$	3	5	7	10
Elapsed Time	71.5	65.5	68.2	66.2

Fig. 10: Computation times of the FRSVT based semi-online weather artifact removal. The elapsed times are measured for a single color channel. Since our algorithm produces  $n$  results simultaneously for  $n$  images at an execution, we report the time for an single image for a single channel. This results show that, when the number of inputs is small, our weather artifact removal algorithm has linear complexity according to the length of a sliding window, thus the elapsed times for a single image are similar.

partial SVD in FRSVT as:  $l = 2$  when  $n = 3$ , and  $l = 3$  when  $n = 5, 7$  and  $10$ . We also apply the power iteration twice, *i.e.*,  $q = 2$ . Our algorithm produces  $n$  results simultaneously for  $n$  images. With an  $n = 5$  sliding window, the method based on SVD takes  $158.9ms$  per a single channel of a  $384 \times 288$  image on Matlab 2014a ( $318.3ms$  on Matlab 2010a), while our method only takes  $65.5ms$ . The qualitative results of our method can be found in Fig. 8, which shows a plausible snow removal effect.

**Type C - Simultaneous Multi-Image Alignment and Rectification** Simultaneous multi-image alignment and rectification problem is Type C optimization suggested by Zhang *et al.* [38] (called SRALT). The method combines the ideas of TILT [39] and RASL [38] on the third-order tensor structure, which exploits low-rank texture property and nuclear norm-based misalignment error, respectively. We show the applicability of FRSVT to NNM on the third-order tensor. We first show that SRALT with FRSVT produces consistent results with the original SRALT on *Digits3* and *Windows* dataset [32] in Fig. 11. Then, we present a new application of SRALT using gait data. We use the parameters  $\alpha$  and  $\lambda$  in Type-C of Table 6 as:  $\lambda = \frac{0.5}{\sqrt{\text{width} \cdot \text{height}}}$ ,  $\alpha = [0.1, 0.1, 0.8]$  for *Digits3* and *Windows*, and  $\alpha = [0.15, 0.15, 0.7]$  for the gait data.

Since gait is a biometric signal spanned on not only spatial domain (2D), but also temporal domain, so it is natural to represent the data by a third-order tensor [24]. In gait recognition, the exact alignment of acquired data is frequently assumed,

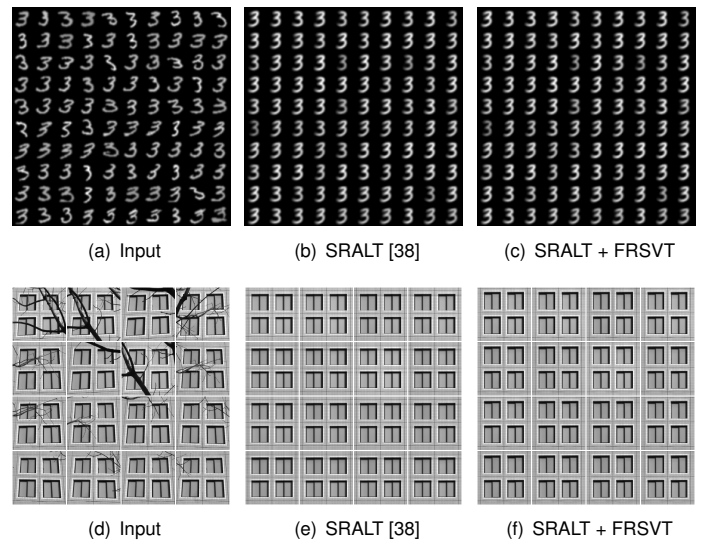


Fig. 11: Qualitative comparisons for the simultaneously alignment and rectification on *Digits3* (top) and *Windows* (bottom) data [32]. The final solutions produce similar results while the computational speed is enhanced by FRSVT.

but in real situations, the accuracy of the gait recognition could be varied depending on the pivot angle of the camera and locations of moving people in both training and test data. Therefore, the SRALT framework is useful to align gait data making sure that the assumption holds and to find a vertical angle as a preprocessing step. We observe that the human silhouettes have the low-rank texture property, and as observed in Lu *et al.* [24], cyclic gait motions are spanned by a few number of bases.

We conduct the experiment using the Gait Challenge data set [35], called USF Human ID version 1.7. There are 731 gait samples and each sample has ten sampled gait cycles, and we only use first 300 gait samples. We resize the images into

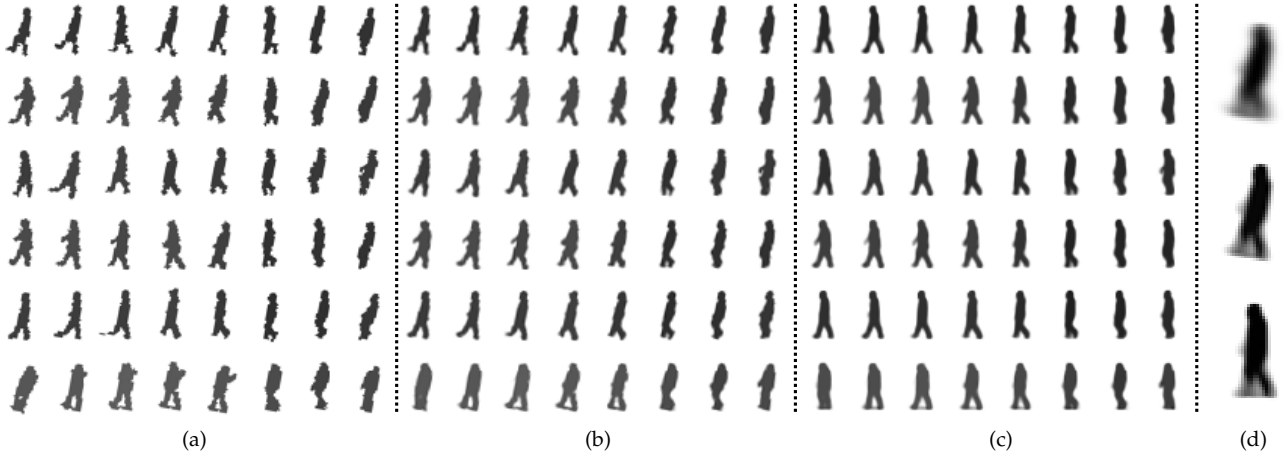


Fig. 12: Qualitative comparison of RASL [32] and SRALT [38] + Our FRSVT. (a) Samples of input images. (b) Results obtained by RASL [32]. (c) Results obtained by SRALT [38] + Our FRSVT. (d) Average images. (Top: for all input images, Middle: for RASL, Bottom: for SRALT+Ours). Due to the angular bias shown in (a), RASL aligns samples to be consistent at the biased angle, while the SRALT based method in (c) not only aligns images, but also corrects upright poses.

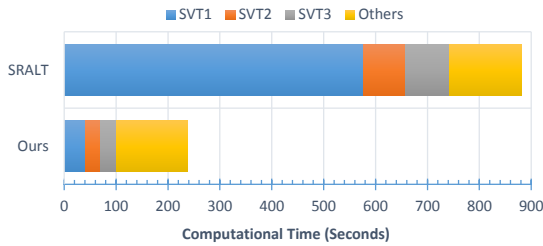


Fig. 13: Computation time comparison on registration and rectification application [38]. The NNM for tensor consists of 3-way SVTs. Computational times are measured for a single outer iteration (almost 100 inner iterations).

$32 \times 22$ , so the size of the input tensor is  $\mathcal{O} \in \mathbb{R}^{32 \times 22 \times 3000}$  (3000 unaligned images with the size  $22 \times 32$ ). The synthetic misalignment generation parameters are described in the below. Randomly drawn Euclidean (3 DoF) geometric transformations are applied to each gait image. The parameters are set to: 1) Scale factor: fixed to 1, 2) Angle noise:  $N(\frac{10\pi}{180}, (\frac{5\pi}{180})^2)$ , 3) Translation noise:  $N(0, 0.5^2) + 2 \cdot (U(0, 1) - 0.5)$ , where  $N(\mu, \sigma^2)$  denotes Gaussian distribution with the mean  $\mu$  and variance  $\sigma^2$ , and  $U(a, b)$  denotes the uniform distribution defined on  $[a, b]$ .

The set of geometric parameters  $\Gamma = \{g_1, \dots, g_{3000}\}$  (see Type C in Table 6) are defined with a  $p$ -group parameterization as  $g_j \in \mathbb{R}^p$ , where 3-DoF parameterization (*i.e.*,  $p = 3$ ) for Euclidean transformation is used in our experiments. We randomly apply translation and rotation to introduce misalignments. Our method is implemented on top of [38] by replacing their SVT method with FRSVT. While the method of [38] is converged at the objective value 206.69 and takes about 6 hours 51 min. (24652s), our method takes only about 1 hour 45 min. (6280s) and reaches the even smaller objective score 206.46. The qualitative and detailed computation time comparisons are summarized in Figs. 12 and 13, respectively.

## 5 CONCLUSIONS

We have presented a fast approximate SVT method that exploits the property of iterative NNM procedures by range propagation and adaptive rank prediction. The approximation error bound shows that our method can produce reliable approximation. The proposed method has been assessed using

the problems of affine constrained NNM, non-convex NNM and NNM on tensor structure as well as the original NNM. The empirical evaluations showed the consistent result with the theoretical analysis, and our approach can reduce the computational time of low-rank applications without losing accuracy and hurting convergence behavior. The major bottleneck of our method is in the power iteration scheme, and we are interested in further reducing the computational complexity by effectively relaxing this computation block in the future.

## REFERENCES

- [1] J.-F. Cai, E. J. Candès, and Z. Shen. A singular value thresholding algorithm for matrix completion. *SIAM Journal on Optimization*, 2010.
- [2] J.-F. Cai and S. Osher. Fast singular value thresholding without singular value decomposition. *Methods and Applications of Analysis*, 2013.
- [3] E. Candès, X. Li, Y. Ma, and J. Wright. Robust principal component analysis? *Journal of the ACM*, 2011.
- [4] Y.-L. Chen and C.-T. Hsu. A generalized low-rank appearance model for spatio-temporally correlated rain streaks. In *IEEE International Conference on Computer Vision (ICCV)*, 2013.
- [5] P. Drineas, R. Kannan, and M. W. Hahoney. Fast monte carlo algorithms for matrices II: Computing a low-rank approximation to a matrix. *SIAM Journal of Computing*, 2006.
- [6] A. Eriksson and A. van den Hengel. Efficient computation of robust weighted low-rank matrix approximations using the  $l_1$  norm. *IEEE Transactions on Pattern Analysis and Machine Intelligence (TPAMI)*, 2012.
- [7] A. Ganesh, Z. Lin, J. Wright, L. Wu, M. Chen, and Y. Ma. Fast algorithms for recovering a corrupted low-rank matrix. In *IEEE International Workshop on Computational Advances in Multi-Sensor Adaptive Processing*, 2009.
- [8] G. H. Golub and C. F. V. Loan. Matrix computations 3rd Ed. *Johns Hopkins University Press*, 1996.
- [9] S. Gu, L. Zhang, W. Zuo, and X. Feng. Weighted nuclear norm minimization with application to image denoising. In *IEEE Conference on Computer Vision and Pattern Recognition (CVPR)*, 2014.
- [10] E. T. Hale, W. Yin, and Y. Zhang. Fixed-point continuation for  $l_1$ -minimization: Methodology and convergence. *SIAM Journal on Optimization*, 2008.
- [11] N. Halko, P.-G. Martinsson, and J. A. Tropp. Finding structure with randomness: Probabilistic algorithms for constructing approximate matrix decompositions. *SIAM Review*, 2011.
- [12] N. J. Higham. Computing the polar decomposition-with applications. *SIAM Journal on Scientific and Statistical Computing*, 1986.
- [13] Y. Hu, D. Zhang, J. Ye, X. Li, and X. He. Fast and accurate matrix completion via truncated nuclear norm regularization. *IEEE Transactions on Pattern Analysis and Machine Intelligence (TPAMI)*, 2013.
- [14] S. Ji and J. Ye. An accelerated gradient method for trace norm minimization. In *International Conference on Machine Learning (ICML)*. ACM, 2009.

- [15] K.-C. Lee, J. Ho, and D. Kriegman. Acquiring linear subspaces for face recognition under variable lighting. *IEEE Transactions on Pattern Analysis and Machine Intelligence (TPAMI)*, 2005.
- [16] Z. Lin. Some software packages for partial svd computation. In *arXiv:1108.1548*, 2011.
- [17] Z. Lin, M. Chen, and Y. Ma. The augmented Lagrange multiplier method for exact recovery of corrupted low-rank matrices. Technical Report UILU-ENG-09-2215, UIUC, 2009.
- [18] Z. Lin, R. Liu, and Z. Su. Linearized alternating direction method with adaptive penalty for low-rank representation. In *Advances in Neural Information Processing Systems (NIPS)*, 2011.
- [19] Z. Lin and S. Wei. A block lanczos with warm start technique for accelerating nuclear norm minimization algorithms. In *arXiv:1012.0365*, 2010.
- [20] G. Liu, Z. Lin, S. Yan, J. Sun, Y. Yu, and Y. Ma. Robust recovery of subspace structures by low-rank representation. *IEEE Transactions on Pattern Analysis and Machine Intelligence (TPAMI)*, 2013.
- [21] G. Liu and S. Yan. Active subspace: Toward scalable low-rank learning. *Neural Computation*, 2012.
- [22] R. Liu, Z. Lin, Z. Su, and J. Gao. Linear time principal component pursuit and its extensions using  $l_1$  filtering. *Neurocomputing*, 2014.
- [23] C. Lu, J. Tang, S. Y. Yan, and Z. Lin. Generalized nonconvex nonsmooth low-rank minimization. In *IEEE Conference on Computer Vision and Pattern Recognition (CVPR)*, 2014.
- [24] H. Lu, K. N. Plataniotis, and A. N. Venetsanopoulos. MPCA: Multilinear principal component analysis of tensor objects. *IEEE Transactions on Neural Networks*, 2008.
- [25] S. Ma, D. Goldfarb, and L. Chen. Fixed point and bregman iterative methods for matrix rank minimization. *Mathematical Programming*, 2011.
- [26] M. W. Mahoney. Randomized algorithms for matrices and data. *Foundations and Trends® in Machine Learning*, 2011.
- [27] Y. Mu, J. Dong, X. Yuan, and S. Yan. Accelerated low-rank visual recovery by random projection. In *IEEE Conference on Computer Vision and Pattern Recognition (CVPR)*, 2011.
- [28] T.-H. Oh, H. Kim, Y.-W. Tai, J.-C. Bazin, and I. S. Kweon. Partial sum minimization of singular values in rpca for low-level vision. In *IEEE International Conference on Computer Vision (ICCV)*, 2013.
- [29] T.-H. Oh, J.-Y. Lee, and I. S. Kweon. High dynamic range imaging by a rank-1 constraint. In *IEEE International Conference on Image Processing (ICIP)*, 2013.
- [30] T.-H. Oh, J.-Y. Lee, Y.-W. Tai, and I. S. Kweon. Robust high dynamic range imaging by rank minimization. *IEEE Transactions on Pattern Analysis and Machine Intelligence (TPAMI)*, 2015.
- [31] T.-H. Oh, Y. Matsushita, Y.-W. Tai, and I. S. Kweon. Fast randomized singular value thresholding for nuclear norm minimization. In *IEEE Conference on Computer Vision and Pattern Recognition (CVPR)*, 2015.
- [32] Y. Peng, A. Ganesh, J. Wright, W. Xu, and Y. Ma. RASL: Robust alignment by sparse and low-rank decomposition for linearly correlated images. *IEEE Transactions on Pattern Analysis and Machine Intelligence (TPAMI)*, 2012.
- [33] G. Pierra. Decomposition through formalization in a product space. *Mathematical Programming*, 1984.
- [34] C. Sanderson. Armadillo: An open source c++ linear algebra library for fast prototyping and computationally intensive experiments. *Technical Report, NICTA*, 2010.
- [35] S. Sarkar, P. J. Phillips, Z. Liu, I. R. Vega, P. Grother, and K. W. Bowyer. The humanoid gait challenge problem: Data sets, performance, and analysis. *IEEE Transactions on Pattern Analysis and Machine Intelligence (TPAMI)*, 2005.
- [36] R. Tron and R. Vidal. A benchmark for the comparison of 3-d motion segmentation algorithms. In *IEEE Conference on Computer Vision and Pattern Recognition (CVPR)*, 2007.
- [37] L. Wu, A. Ganesh, B. Shi, Y. Matsushita, Y. Wang, and Y. Ma. Robust photometric stereo via low-rank matrix completion and recovery. In *Asian Conference on Computer Vision (ACCV)*, 2010.
- [38] X. Zhang, D. Wang, Z. Zhou, and Y. Ma. Simultaneous rectification and alignment via robust recovery of low-rank tensors. In *Advances in Neural Information Processing Systems (NIPS)*, 2013.
- [39] Z. Zhang, A. Ganesh, X. Liang, and Y. Ma. TILT: Transform invariant low-rank textures. *International Journal of Computer Vision (IJCV)*, 2012.
- [40] Y. Zheng, G. Liu, S. Sugimoto, S. Yan, and M. Okutomi. Practical low-rank matrix approximation under robust  $l_1$ -norm. In *IEEE Conference on Computer Vision and Pattern Recognition (CVPR)*, 2012.



the IEEE.

**Tae-Hyun Oh** received the B.E degree (summa cum laude) in Computer Engineering from Kwang-Woon University in 2010, and the M.S degree in Electrical Engineering from KAIST in 2012. He is currently working towards the Ph.D. degree at KAIST, South Korea. He was a visiting student in the Visual Computing Group, Microsoft Research Asia. He was a recipient of Gold prize of Samsung HumanTech Thesis Award and Qualcomm Innovation Award. His research interests include robust computer vision and machine learning. He is a student member of



**Yasuyuki Matsushita** received his B.S., M.S. and Ph.D. degrees in EECS from the University of Tokyo in 1998, 2000, and 2003, respectively. From April 2003 to March 2015, he was with Visual Computing group at Microsoft Research Asia. In April 2015, he joined Osaka University as a professor. His research area includes computer vision, machine learning and optimization. He is on the editorial board of IEEE Transactions on Pattern Analysis and Machine Intelligence (TPAMI), International Journal of Computer Vision (IJCV), IPSJ Journal of Computer Vision and Applications (CVA), The Visual Computer Journal, and Encyclopedia of Computer Vision. He served/is serving as a Program Co-Chair of PSIVT 2010, 3DIMPVT 2011, ACCV 2012, ICCV 2017, and a General Co-Chair for ACCV 2014. He is a senior member of IEEE.



**Yu-Wing Tai** received the Ph.D. degree from the National University of Singapore (NUS) in June 2009. He joined KAIST, South Korea, as an assistant professor in Fall 2009. He regularly serves on the program committees for the major Computer Vision conferences (ICCV, CVPR and ECCV). His research interests include computer vision and image/video processing. He is a senior member of the IEEE.



**In So Kweon** received the BS and MS degrees in mechanical design and production engineering from Seoul National University, in 1981 and 1983, respectively, and the PhD degree in robotics from Carnegie Mellon University, 1990. He is now a professor at KAIST, South Korea. He is a recipient of the best student paper runner-up award at CVPR 09'. He was the program chair for ACCV 07' and is the general chair for ACCV 12'. He is also on the editorial board of the IJCV.